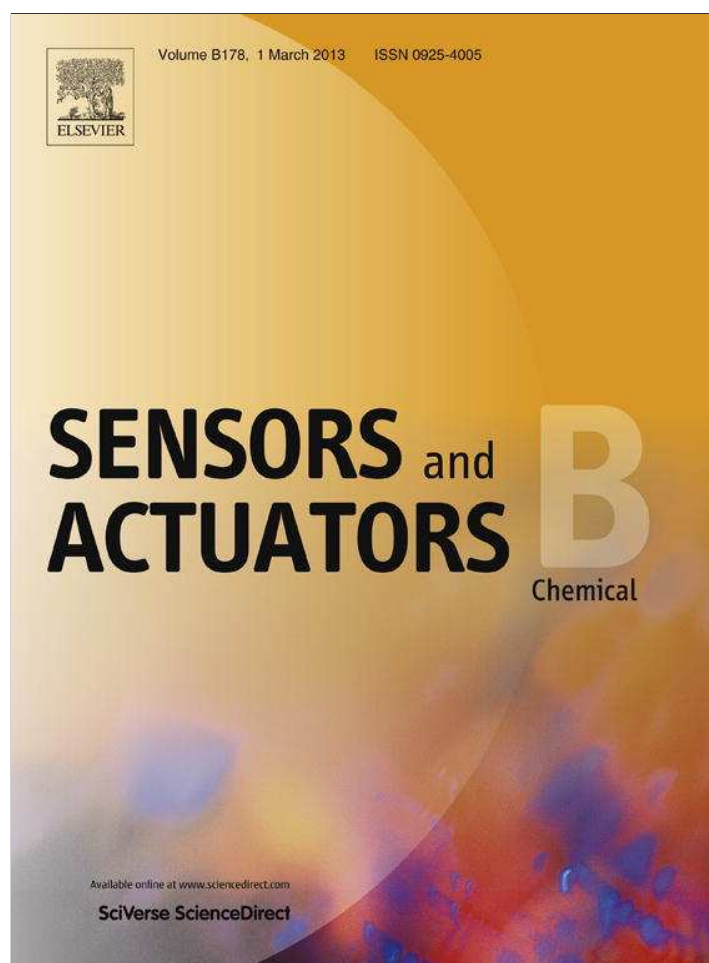


Provided for non-commercial research and education use.
Not for reproduction, distribution or commercial use.



This article appeared in a journal published by Elsevier. The attached copy is furnished to the author for internal non-commercial research and education use, including for instruction at the authors institution and sharing with colleagues.

Other uses, including reproduction and distribution, or selling or licensing copies, or posting to personal, institutional or third party websites are prohibited.

In most cases authors are permitted to post their version of the article (e.g. in Word or Tex form) to their personal website or institutional repository. Authors requiring further information regarding Elsevier's archiving and manuscript policies are encouraged to visit:

<http://www.elsevier.com/copyright>



Contents lists available at SciVerse ScienceDirect

Sensors and Actuators B: Chemical

journal homepage: www.elsevier.com/locate/snb

Review

Cell electrofusion in microfluidic devices: A review

Ning Hu^{a,b}, Jun Yang^{a,*}, Sang W. Joo^{b,*}, Arghya Narayan Banerjee^b, Shizhi Qian^{b,c,*}^a Key Laboratory of Biorheological Science and Technology, Ministry of Education, Key Laboratory for Optoelectronic Technology and Systems, Ministry of Education, Chongqing University, Chongqing 400030, PR China^b School of Mechanical Engineering, Yeungnam University, Gyongsan 712-749, South Korea^c Institute of Micro/Nanotechnology, Old Dominion University, Norfolk, VA 23529, USA

ARTICLE INFO

Article history:

Received 8 October 2012

Received in revised form 2 December 2012

Accepted 8 December 2012

Available online 19 December 2012

Keywords:

Cell

Pairing

Electrofusion

Electroporation

Dielectrophoresis

Microfluidics

ABSTRACT

Cell electrofusion in microfluidic devices attracted great attention in recent years due to its widespread applications potential in cell-based studies. In these microfluidic devices, many manipulation methods, such as chemical conjugation, electric field induced dielectrophoresis, and microfluidic controlling based on microstructure, are used to improve the pairing precision of cells, especially heterogeneous cells. High-strength electric field can produce minipores on cell membrane and induce cell fusion. It can be generated by a constricting electric field with microstructures or two microelectrodes. In comparison with the traditional electrofusion or other cell-fusion methods, microfluidic cell-electrofusion method has many advantages such as precise manipulation, high efficiency in cell pairing and fusion, higher cell viability, lower sample contamination and smaller Joule heating effect. In this article, the development of various microfluidic cell-electrofusion methods is reviewed. Some important parameters affecting the cell electrofusion are discussed in detail. Techniques that can be integrated on microfluidic devices for high-efficiency cell electrofusion, such as on-chip cell separation and culture, are also discussed comprehensively.

© 2012 Elsevier B.V. All rights reserved.

Contents

1. Introduction	64
2. Cell pairing	64
2.1. Cell pairing by chemical method	65
2.2. Cell pairing by electric field	66
2.2.1. Field modification/enhancement by microelectrode geometry	66
2.2.2. Field modification/enhancement by microstructure between electrodes	68
2.3. Cell pairing by microstructure	70
3. Cell reversible electroporation	74
3.1. Cell reversible electroporation induced by microelectrodes	74
3.2. Cell reversible electroporation induced by electric field constriction	75
4. Other important factors affecting the performance of cell electrofusion	78
4.1. Geometry and material of microelectrodes	78
4.2. Electronics signal	80
4.3. Cell types	81
4.4. Osmolarity of buffer solution	81
5. Future trends	82
6. Conclusions	83
Acknowledgement	83
References	83
Biographies	85

* Corresponding authors.

E-mail addresses: bioyangjun@cqu.edu.cn (J. Yang), swjoo@ynu.ac.kr (S.W. Joo), sqian@odu.edu (S. Qian).

1. Introduction

Recently, nucleus transfer [1], hybridoma [2], production of cloned offspring [3–6], and the epigenetic reprogramming of somatic cells [7–10] attract many attentions. Cell fusion is one of the most important methods that can produce new intercellular genetic materials, where mediating and culturing methods are applied to merge two or more cells into a hybrid cell in an asexual way [11]. The hybrid cell obtains genetic materials from two parent cells. In addition to aforementioned applications, it also can be used in genetics [12,13], immunology [14–20], developmental biology [21], drug/gene delivery [22,23], hybridization/crossbreeding studies [6,24–28], among others [29,30]. Compared with biological [31] and chemical fusion methods, in which some hazardous exogenous materials such as inactivated virus [32,33] or polyethylene glycol (PEG) [34] are introduced, the electrofusion has considerable advantages, including easy operation, low toxicity and widespread adaptability. In addition, the efficiency of electrofusion is usually much higher than the PEG-based approach [26,35–40].

The traditional cell-electrofusion process, which was firstly developed by Zimmermann [35], can be divided into four consecutive steps: (i) cell alignment/pairing by positive dielectrophoresis (the electric field strength: 100–300 V/cm) or other methods, such as laser-based single cell manipulation [41–43], (ii) reversible electroporation on cell membrane under high-strength direct current (DC) pulses (1–10 kV cm⁻¹), (iii) membrane reconstruction and cytoplasm exchange between two cells, and (iv) nucleus fusion and hybrid cell formation. In the cell electrofusion process, cell pairing and reversible electroporation play important roles for the formation of final products. Original cell electrofusion system used a fusion chamber with two parallel wire electrodes of 0.1–0.2 mm spacing as reactors. In addition, helical chamber and fusion chamber with two wide-distance parallel electrodes (0.1–20 mm) are also developed for large-scale electrofusion [44]. Therefore, a high-voltage power supply is required to generate electric field strong enough for reversible electroporation on the cell membrane. Moreover, it is difficult to avoid the formation of multi-cell fusion in traditional electrofusion systems because similar membrane potential at each cell junction point within a long cell chain results equal probability of reversible electroporation and fusion [45]. It is also difficult to separate the hybrids from multi-cell fusion by existing cell separation methods, including fluorescence activated cell sorter (FACS), magnetic-activated cell sorting (MACS), and hypoxanthine–aminopterin–thymidine (HAT) screening. Moreover, large-scale electric field in traditional cell-electrofusion systems cannot precisely manipulate cells, and so high-precision cell pairing and high-efficiency cell electrofusion cannot be achieved.

With the development of microfabrication techniques, different types of microelectrodes and microstructures are integrated on microfluidic chips to solve the aforementioned problems by shortening the distance between the two microelectrodes or by constricting the electric field. Most existing studies focus on the two steps of the cell-electrofusion process, *i.e.* the cell pairing and cell electroporation [46,47]. Different methods used to improve these two processes are schematically shown in Fig. 1. In general, three methods, namely chemical conjugation, dielectrophoretic force (field modification/enhancement by microelectrode geometry or microstructure between electrodes) and field-free microstructures trapping (such as micro-traps, flow control *etc.*), have been used in cell pairing, whereas cell electroporation is induced by controlling the geometry of the microelectrodes or microstructures within the microfluidic devices. In the chemical conjugation method of cell pairing, two cells can be chemically conjugated by lectin or biotin–streptavidin interaction with high throughput [48,49]. However, this method lacks the ability of pairing

unmodified cells. In addition, the random conjugation may induce undesired pairing. To overcome these difficulties, dielectrophoretic force, generated by optimized microelectrodes, is applied to enhance the cell-pairing efficiency. However, the dielectrophoretic force by itself cannot realize precise pairing of two heterogeneous cells like A–B type with high efficiency. The combination of microstructures, like micro-orifice/micro-trap/micropit, with other controlling methods, such as hydrodynamic pressure/gravity/dielectrophoretic force, is developed for manipulating the pairing process of heterogeneous cells. Due to the short distance between the microelectrodes or the electric field constriction, a low voltage is sufficient to achieve cell electrofusion in microfluidic cell-electrofusion devices, and thus can reduce the cost of high-voltage power generators as well as the negative effect of Joule heating present in traditional cell-electrofusion systems. Besides the cell pairing and electrofusion, the cell separation and cell culture are also indispensable manipulations for the cell-fusion research, but are not considered in most microfluidic electrofusion devices.

Since the cell pairing and cell electroporation methods are considered to be the two most important steps for electrofusion, a comprehensive review of the existing processes and current trends in these fields warrants considerable attention. And therefore, in this article, we have presented a detailed review of the latest achievements of the chip-based cell electrofusion as follows:

- Firstly, cell pairing in microfluidic devices is discussed in detail. Different methods used to obtain high heterogeneous cell pairing efficiency, such as electric field manipulation, chemical conjugation and microstructure trapping, are discussed in terms of improved cell pairing processes.
- Secondly, reversible electroporation on microfluidic devices is presented in detail. Various methods used to generate high-strength localized electric field in terms of optimization of the geometry of microelectrodes/microstructures *via* electric field constriction effect are discussed.

In order to understand the functionality and performance of these microfluidic devices better, various methods used for cell pairing and cell electroporation are compared as well. Additionally, some novel microfluidic cell electrofusion devices using suitable combination of aforementioned cell pairing and cell reversible electroporation methods are described. In addition, the influences of some important factors on the overall electrofusion process, such as the material and shape of the electrodes, cell types, osmolarity of buffer solution *etc.* are also discussed in detail. Finally, the shortcomings of the existing microfluidic cell electrofusion are summarized, and some trends and guidelines are proposed for future works.

2. Cell pairing

It is well known that stable pairing of cells is the basis for electrofusion. In order to obtain high fusion efficiency, high efficiency in cell pairing is required. In conventional research, cell fusion is accomplished in a fusion chamber by high speed centrifugation [50], chemical induction [51,52] and dielectrophoresis to perform cell pairing [38,53–56]. However, these methods are in general based on a random cell contact, and cannot control the number of cell chains. It results in low pairing efficiency, especially for the two-cell pairing and the pairing of heterogeneous cells. The paired cells include the types of AA, BB, and AB, among which only AB is the desirable type for cell fusion. Some complex detection or separation techniques, such as FACS, MACS, HAT screening, are developed for isolating AB cells from the cell suspension. Moreover, high-ratio alignment/pairing of multiple cells will produce many undesirable

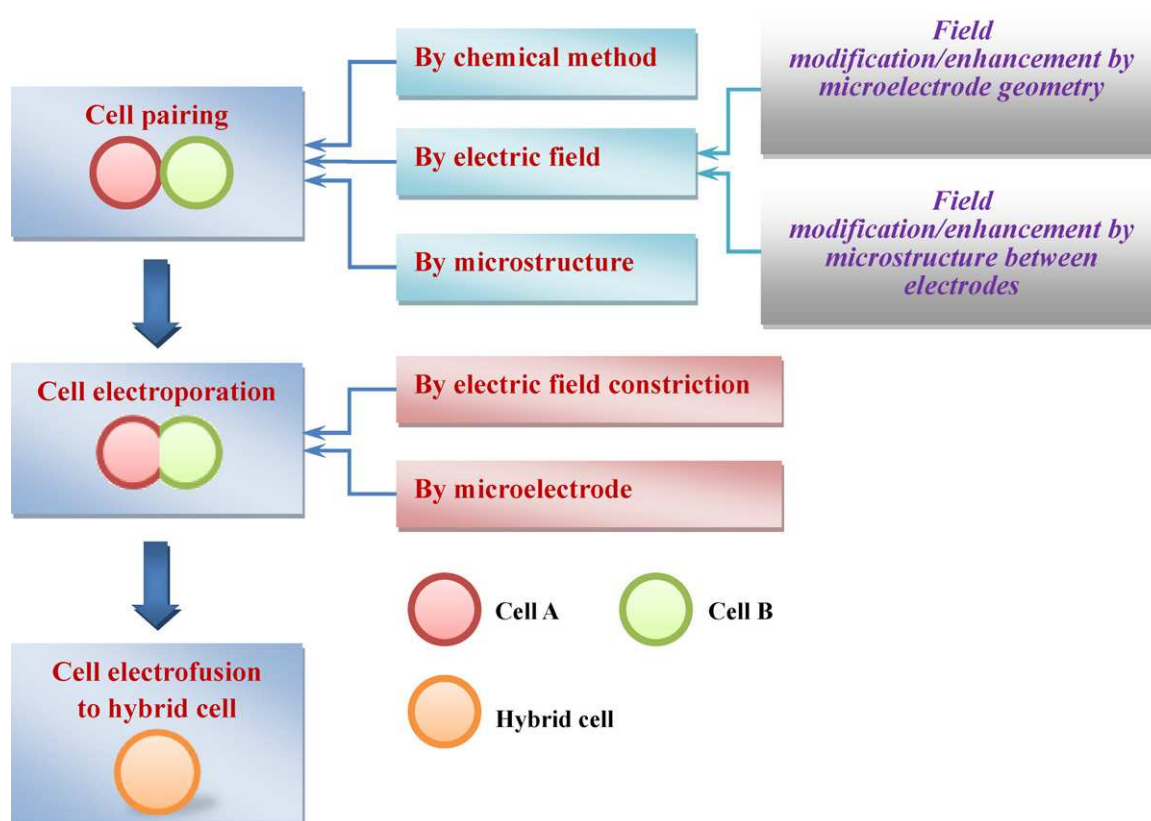


Fig. 1. Schematic flow-chart representing different cell-pairing and cell-electroporation methods used for cell-electrofusion.

hybrid cells with multi-nucleus due to multi-cell fusion which include ABB, BBA, or AABB types of hybrid cells, which are difficult to be selected and separated from AB cell suspension by the conventional screening methods mentioned above.

Recent microfluidic technology allows fabrication of microstructures with a size similar to the characteristic scale of biological cells, and thus enables researchers to perform electrofusion experiments in micro-scale. The microfluidic technology can provide more specific manipulation tools as well, such as micro-scale electric field and microstructure, for cell pairing in high efficiency and high precision. As mentioned earlier, cell pairing is generally performed by three techniques: by using chemical method, by electric field (DEP), or by trap microstructures. Each of these methods is discussed in detail below.

2.1. Cell pairing by chemical method

Generally, standard microfluidic-based cell-electrofusion requires multiple voltage sources consisted with AC and DC generators, where the AC source (low voltage) provides the cell-pairing and the DC source (high voltage) realizes the cell-electroporation [57]. Obviously it creates complex instrumentation, and reduces cost-effectiveness. To overcome this problem, several groups used a chemical method for cell pairing, which obviates the use of dual power supplies, requiring only a common DC source on the microfluidic platform. This novel chemical pairing method with high heterogeneous cell pairing efficiency is developed based on various chemicals like biotin–streptavidin and lectin-couplet, among others. Wang and Lu [48] have used biotin–streptavidin chemical linking, which is based on the biomolecular interaction [58]. By biotinylated linked conjugation reagent, two types of cells can create the cross-linking. Based on biotin–streptavidin interaction, one half of the cell sample was labeled/biotinylated

by Sulfo-NHS-LC-biotin, whereas the other half of the cell sample was treated for streptavidin coating after biotinylation. Under the conjugation mode of cell-biotin–streptavidin–biotin-cell, about 50–55% cell population was conjugated by this chemically linked protocol after mixing and incubation. In addition, more than half of these cell-pairs (about 30% of cell sample) are found to be one-to-one conjugation. Apart from the simplicity of instrumentation, as mentioned above, the advantages of this method include no damage of the cell membrane, and high effectiveness of pairing of two different types of cells (even with significantly different diameters).

Besides using biotin–streptavidin chemical conjugation method, zona-free cytoplasts were attached by using lectin to somatic or embryonic donor cells to conduct cell pairing for nuclear transfer cloning in cell fusion [59,60]. Firstly, these cells were loaded into a mouth pipette with drops of 20 $\mu\text{g}/\text{ml}$ phytohe-magglutinin (PHA-P) in Heps-buffered tissue culture medium 199 (H199) containing 5–10 cytoplasts. After mixing the cytoplasts and donor cells, incubation of the mixture solution for a few minutes (~ 5 min) was performed, followed by washing in H199+ bovine serum albumin (BSA, 3 mg/ml), which resulted in the formation of the zona-free couplet. As mentioned above, by using chemical conjugation pairing method, cells with widely varied diameters can be paired. For example, Clow et al. [49] reported the pairing of cytoplast, having large diameter ($\sim 118 \mu\text{m}$), with fetal fibroblast donor having a relatively small diameter ($\sim 13 \mu\text{m}$). Also this method offers a relatively higher throughput in cell pairing compared to the electric field/microstructure-induced cell-pairing processes (described later). This is because these latter methods have the limitation in the integration of number of microelectrodes/microstructures within the microfluidic devices through the conventional lithography-based fabrication methods. However, this chemical conjugation method of cell pairing suffers from some disadvantages. For example, since this process requires

a pre-modification treatment of each cell sample prior to the cell pairing, this chemical pre-treatment tends to modify the membrane structure of cell sample, leading to potential damage on cell viability. Moreover, the cell pairing between one A cell and two or more B cells (or *vice versa*) cannot be avoided by this method due to the random cell contact, especially within a mixture of cells with significantly different diameters. Therefore, the one-to-one pairing and the heterogeneous cell pairing efficiency are not very high.

2.2. Cell pairing by electric field

Cell pairing by electric field is based on electrophoretic manipulation and interaction of polarized cells [61]. Mostly, cell pairing in microfluidic devices always uses positive dielectrophoretic force to trap and pair cells. Dielectrophoresis is a particle movement induced by the polarization effects in non-uniform AC or DC electric field [62], which was first discovered by Pohl and Crane in 1951 [63]. As the dielectrophoretic force has been used for capturing and pairing cells in cell fusion since 1980, this manipulation technology has widespread applications [64–66] due to easy operation, precise controllability of the dielectrophoretic force through field-parameter adjustments [65], and easy integration with other manipulation techniques [67]. Also this method eliminates the complex pre-modification treatments used in chemical conjugation method mentioned earlier. Moreover, cells in the captured regions near microelectrodes can be paired with any cells. Thus, this method can improve the adoption of different cells. Also cells in the microchannel can move to the high electric field area, and create cell pairing under positive DEP force induced by the non-uniform electric field distribution. The high-strength non-uniform field distribution can be produced by two ways. The first one is by using specially fabricated microelectrodes where the electrode geometry plays an important role to produce non-uniform electric field distribution in such a way that the field becomes higher near the microelectrodes with respect to the other positions. On the other hand, fabrication of microstructures with some dielectric material within the microfluidic device can also produce non-uniform electric field distribution within the micro-channel. With judicious placement of these insulating microstructures between the microelectrodes, electric field can be enhanced locally on some pre-selected areas of the micro-channel *via* electric field constriction effect. The two methods of generating non-uniform field mentioned above are described in the following sub-sections. Besides positive dielectrophoretic force, negative dielectrophoretic field was also used to manipulate cells, like cell sorting, trapping and collection. In addition, negative dielectrophoretic force applied in cell trapping and formation of cell aggregates attracted great attentions [68–70]. Moreover, the low-strength electric field surrounding environment for cell couplets is helpful for cellular vitality [71,72].

2.2.1. Field modification/enhancement by microelectrode geometry

Microelectrode-assisted cell pairing is a method that uses specially designed microelectrodes to produce non-uniform electric field distribution in microfluidic channel. Generally, the electric field strength near the microelectrode is much higher. Cells in the microchannel will move and attach to the microelectrodes, and realize cell alignment due to the positive dielectrophoresis.

In the last decade, several groups [73–83] designed protruding microelectrodes for cell pairing and electrofusion. Tresset and Takeuchi [74] developed a microfluidic device for electrofusion of biological vesicles, based on a 250 μm thick low-resistance silicon wafer (resistivity $<0.01 \Omega\text{cm}$) bonded to glass substrate. Fig. 2a represents the schematic diagram of the microfluidic platform reported by Tresset and Takeuchi [74]. As shown in the

figure, the microelectrode arrays are fabricated to protrude into the microchannel, and hence played the role of sidewall of the channel. Therefore, it also improves the integration of microelectrodes in microfluidic channel. The widths of the microfluidic channel are varied from 500 to 30 μm . A 300 kHz, 0.1–0.2 kV cm^{-1} AC electric field was used to drive liposomes/cells for cell alignment/pairing process. Due to the special geometry of the electrode arrays, a non-uniform electric field is generated within the channel having higher field gradient near the side-wall surface of the protruding electrodes. This enhances the probability of the cell alignment and pairing at the sidewall of protruding electrodes. Using a similar designing protocol, Yang et al. [76,81] fabricated a microfluidic chip with thousands of protruding microelectrodes on a SOI wafer for high throughput electrofusion. This cell-electrofusion chip is consisted with six microchambers. In order to integrate more electrodes, each microchamber contains two serpentine-shaped microchannels. The depth and width of these microchannels are 20 and 80 μm , respectively. The geometric parameters of these microelectrodes are same in different chambers, while the distance between two opposite microelectrodes varied from 50 to 100 μm with an increment of 10 μm in each chamber. This design allows the chips to have high adoptability in fusing cells with different diameters. The AC electric field (0.8–1.2 kV cm^{-1} , 1 MHz) applied on the microelectrode array produces a dielectrophoresis force, and drives cells to pair. In addition, the cell pairing result shows that the length of the cell alignment chain can be controlled by the AC electric field strength. Similarly, Qu et al. [83] fabricated 5000 asymmetric protruding microelectrodes on a 1.5 cm \times 1.5 cm glass-silicon bonding wafer. The specific protruding microelectrode configuration created an effective region for cell alignment in about 2–4 cellular size by adjusting the applied voltage and the distance between two counter protruding microelectrodes. Under the dielectrophoretic force, a major proportion of the cells ($\geq 95\%$) were attracted toward the edge of microelectrodes for docking. The optimal region of cell alignment is wider than the size of two cells and narrower than the size of three cells. Accordingly, the distance between two counter protruding microelectrodes should be the size of 4–5 cells suitable for two-cell alignment. Experimental results show that about 42–68% cells aligned as cell–cell pairs. And the pairing ratio of heterogeneous cells is about 35% as depicted in the microscopic image (cf. Fig. 2b, red dotted circles), indicating higher efficiency of cell pairing through this fabrication protocol.

One disadvantage of the protruding microelectrode structure is that it forms cavity area between two adjacent microelectrodes (also called “dead area”) and cells are found to be easily trapped in these areas during loading and cell alignment process, as indicated by white circles in Fig. 2b). As the electric fields in these areas are lower than other areas, it affects the reversible electroporation, leading to a decrement in the overall electrofusion efficiency. To overcome this problem, Hu et al. [75] presented a discrete microelectrodes array structure based on the thin film microelectrode. This microfluidic chip is fabricated on a quartz glass substrate, which consists of a serpentine-shaped microfluidic channel made of insulation material (Durimide 7510), a sandwich structure consisting of a chiasma-shaped thin film microelectrode array (from bottom to top), 1015 pairs of discrete thin film microelectrodes deposited on each sidewall of the microfluidic channel, and another chiasma-shaped thin film microelectrode array. On this microfluidic chip, the electric field distribution is non-uniform and similar to the protruding microelectrodes mentioned previously. But the main advantage in this current device is that it also keeps a smooth microfluidic channel wall because the thickness of Au thin film is only 0.3 μm . Compared to the protruding microelectrode structure described previously, the filling of the “dead areas” between two adjacent microelectrodes by the dielectric material (Durimide 7510) in this device nullifies the presence of electric

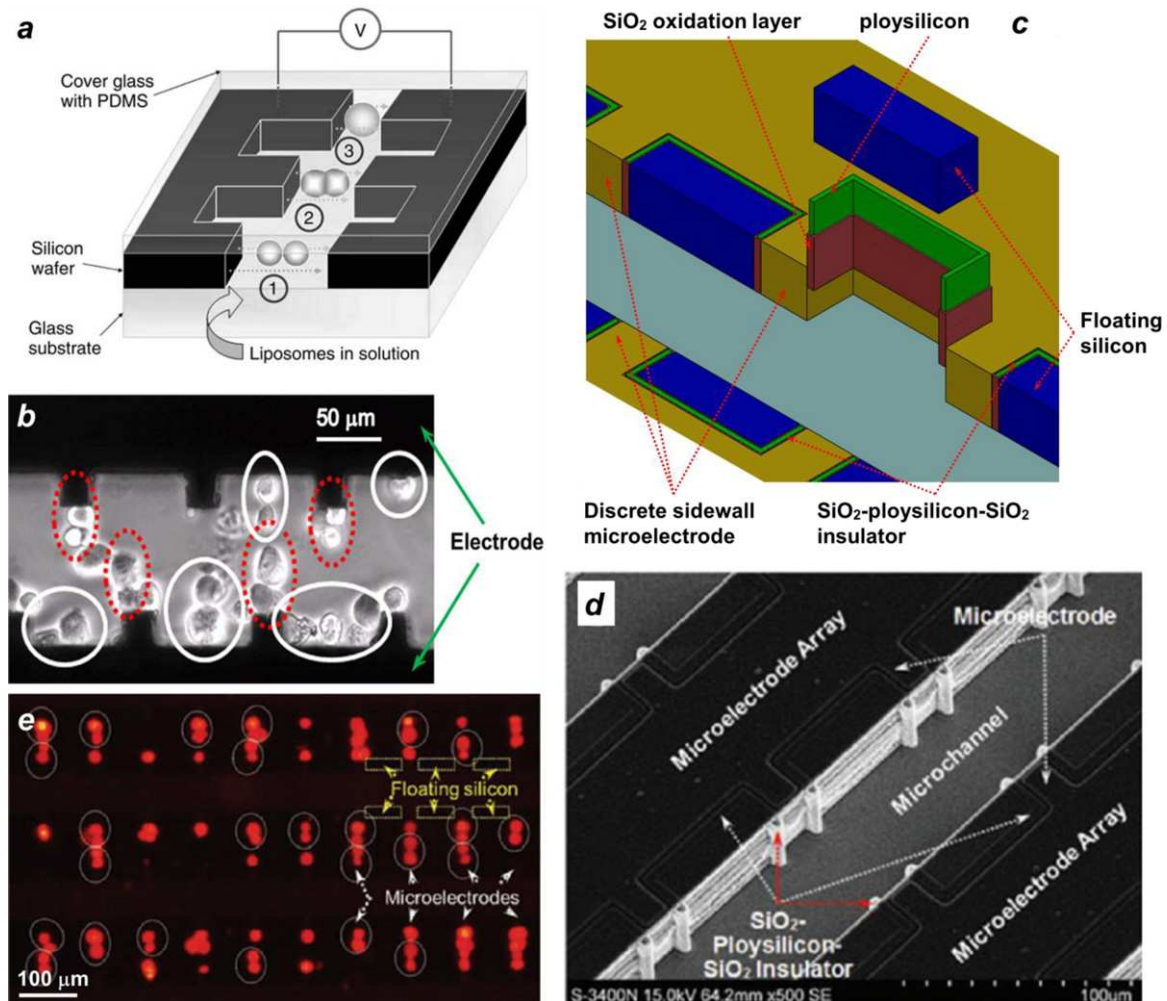


Fig. 2. Schematic structure of protruding microelectrodes for cell pairing on microfluidic chip. (a) The fusion protocol starts with highly efficient cell pairing near the protruding electrodes (1), followed by electroporation (2), and fusion (3) [74]. (b) Cell alignment in a microchannel with protruding microelectrode array (Red dotted circles show cell-pairing at the edge of the protruding microelectrodes, while white solid circles show that some cells are trapped in the gaps ['dead areas'] between two adjacent protruding microelectrodes). (c) Schematic diagram of microfluidic device based on SiO_2 -Polysilicon- SiO_2 structure and discrete microelectrodes. (d) The view of the actual cell electrofusion microfluidic chip (SEM 200 \times). (e) Image of the NIH3T3 cell alignment in the microfluidic chip. Adapted with permission from Ref. [82]. (For interpretation of the references to color in this figure legend, the reader is referred to the web version of the article.)

signal in these areas, leading to almost negligible cell trapping in the 'dead areas.' It is observed that more than 99% cells are successfully trapped at the edges of the discrete microelectrodes, and about 70% cells are aligned as cell-cell pairs. It shows a great improvement over the previously described protruding microelectrode array (whose efficiency is only about 40%). Besides the thin film discrete microelectrodes, discrete coplanar vertical sidewall microelectrodes (cf. Fig. 2c and d) are also developed by Hu et al. [82] based on a SOI wafer to eliminate the "dead areas." Adjacent microelectrodes on each sidewall are separated by coplanar SiO_2 -polysilicon- SiO_2 /silicon and floating silicon structure, which filled the "dead areas." A schematic structure of the device is shown in Fig. 2c, whereas the actual image of the device is represented in Fig. 2d. Since the floating silicon without electric signal cannot induce positive DEP force, cells cannot move and pair on it. About 100% cells are observed to be aligned to the discrete microelectrodes. Cell-cell pairing efficiency is also found to be around 70% (as shown in Fig. 2e). However, some cell chains are found to contain one cell or more than 2 cells and the pairing of two types of cells as AB is still random.

To obtain more specific manipulation in cell pairing, microfluidic control was used to assist dielectrophoretic cell pairing. A microfluidic chip, consisted with a polydimethylsiloxane

(PDMS)-based microchannel with a fusion chamber and two opposite gold-titanium (Au-Ti) electrodes, was developed by Ju et al. [80]. This microfluidic device combined the dielectrophoretic force and hydrodynamic force, and realized high cell pairing efficiency on plant cells. In this device, samples are continuously fed through the regions within microelectrodes by a pressure-driven flow with the imposed differential pressure between the inlet and outlet of the device (cf. Fig. 3a). An AC electric field is applied between the opposite microelectrodes, and cells are paired at the microelectrodes by the induced positive DEP under appropriate differential pressure. The optimal AC electric field for pairing (amplitude: 0.4–0.5 kV cm^{-1} , frequency: 1.5 MHz) is determined after obtaining the variation of the pearl chain ratio of five kinds of plant cells. With a low flow rate (flow speed within the fusion chamber $<40 \mu\text{m s}^{-1}$), $92 \pm 2.3\%$ of the cells are trapped by the electrodes. As the fluid velocity increases, the number of cells trapped by the microelectrodes decreases, as shown in Fig. 3b–d. The cell-cell pairing on this microfluidic chip is higher than traditional pairing protocol. In addition, after the capture of the first cell on the microelectrodes, second type of cell can be injected into the microfluidic channel. Under suitable double forces, two types of cells can pair in one-to-one heterogeneous conjugation method. However, the flow velocity is hard to control to realize the capturing of just two cells

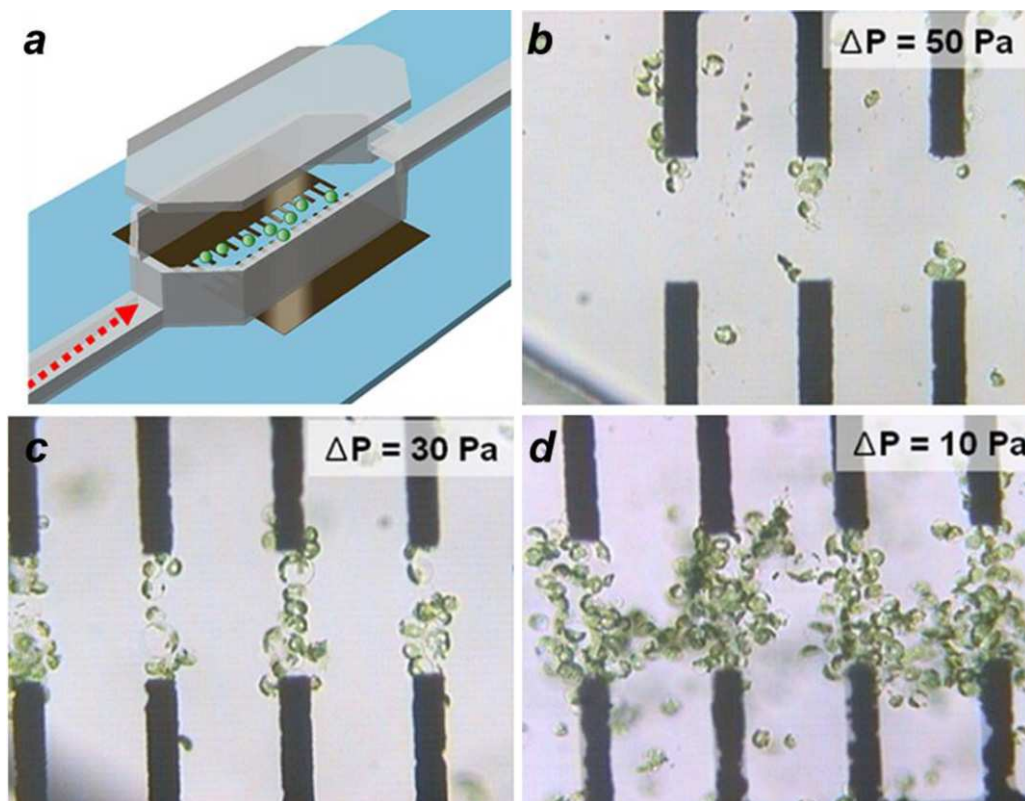


Fig. 3. Schematic structure of the microfluidic device and cell pairing under different pressure gradient (ΔP). (a) Schematic diagrams of the 3D electrofusion chip: dimensions of the microfluidic channel (H : 0.2 mm, W : 0.1 mm, L : 17 mm), fusion chamber (H : 0.6 mm, W : 0.6 mm, L : 2 mm). (b–d). The dependence of the pearl chain formation rate on the differential pressure: (b) the differential pressure is 50 Pa; (c) 30 Pa. (d) 10 Pa. Adapted with permission from Ref. [80].

at each microelectrode, especially when the sizes of the cells are significantly different, as both the dielectrophoretic force and the hydrodynamic force depend on the size of the cells. It also induces low heterogeneous cell pairing efficiency.

Besides Positive dielectrophoretic force, negative dielectrophoretic (nDEP) force has also been used in cell pairing process [84,85]. Kirschbaum et al. [71] developed a single-cell level electrofusion microfluidic device, which allowed gentle and contact-free cell manipulation in standard cell culture medium. In this microfluidic device, two kinds of cell suspensions, Myeloma cells and B cell blasts, are introduced into the microfluidic channel by two separated inlets. The two cells under consideration, either homologous or heterologous, are selected by the switch electrodes. Subsequently, these two cells are transported to a central processing area (CPA) by the hydrodynamic flow and the dielectrophoretic force, induced by deflection electrodes. Considering the geometry of zigzag electrodes, electrical parameters of surrounding medium and cells, nDEP force induced by AC signal retains cells against the flow, and traps them at the zigzag electrode area. In addition, these two cells are paired by the mutual inactivation between two polarized cells. This method is also used in cell pairing between cells and beads, and multi-cell pairing applications. It shows specific manipulation in the cell selection and pairing between two types of cells, and good adaption in rare cell electrofusion.

2.2.2. Field modification/enhancement by microstructure between electrodes

Besides using microelectrodes of different geometries to induce positive DEP force for cell pairing, construction of micro-structure within the microchannel [46,86–89] can also modify the electric field spatial distribution and produce positive DEP force to attract and pair cells with high efficiency. Generally, the micro-structures

are fabricated by dielectric material within the microfluidic channel in such a way that the electric field is concentrated at some specific areas. Cells in the microfluidic channel is then driven by the induced positive DEP force, and paired at these positions with higher electric field.

In 1989, Masuda et al. [86] developed a microfluidic chip for electrofusion which consists of a fusion chamber and a pair of parallel electrodes. The chamber was divided into two microfluidic channels by an insulated wall that contained a small opening. Due to this specially designed microstructure, majority of the electric-field lines were concentrated at the small opening to produce a strong electric field constriction area between two opposite microelectrodes. Cells A and B were loaded into the respective channel. When these cells were allowed to flow through the fusion chamber, AC voltage (2 MHz, variable-voltage: 0–30 V) was applied on the electrodes that produced high electric field at the insulator opening. Cells A and B then moved towards the high electric field zone (the center of small opening), and formed cell pearl-chain A–B at this point, under the positive dielectrophoretic force, as shown in Fig. 4.

However, the above-mentioned microfluidic device suffers from one disadvantage, which is the low throughput of cell pairing because of the limitation in microelectrodes and small opening. To overcome this shortcoming, Gel et al. [46] recently fabricated a microfluidic chip, which was composed of a glass substrate, a fusion chamber, and two opposite electrodes. The fusion chamber was divided into two microfluidic channels by the micro-orifice array partition located in the middle of the fusion chamber. Each microfluidic channel contained an inlet for cell loading. In cell pairing process, two suspensions with different cell types were introduced into each inlet and filled the microfluidic channels. Firstly, the chip was tilted to create a flow under hydrostatic

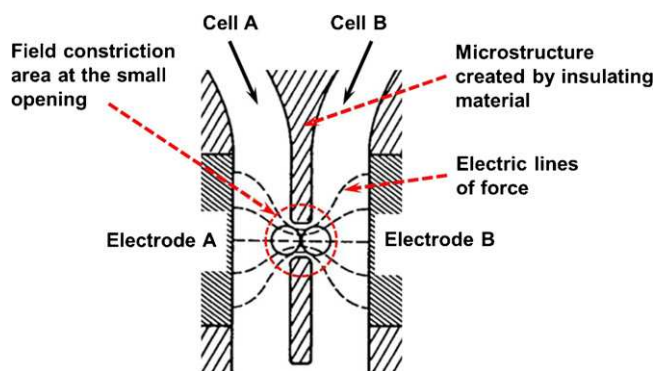


Fig. 4. Schematic of electric field constriction and two type cells pairing on the micro-opening. Adapted with permission from Ref. [86].

pressure, and carried one type of cells (cell A) toward the micro-orifice. After that, an AC signal was applied on the two opposite electrodes to produce a dielectrophoretic force. Since the micro-orifice concentrated the electric field lines and generated high electric field zone under positive dielectrophoretic force, cells A moved to the high electric field zones and were trapped at the micro-orifice when the chip was tilted the other way. Cells B in the other side of fusion chamber were also moved to the micro-orifice under the hydrostatic pressure and the dielectrophoretic force. Cells A and B made contact through the micro-orifice, and formed pairs, as shown schematically in Fig. 5a, whereas an SEM image of the micro-orifice structure is shown in Fig. 5b. This pairing protocol can avoid the mixing of different types of cells by using the partition structure. And the pairing efficiency can reach almost 95–100%, as shown in the real-time microscopic image in Fig. 5c.

Although the aforementioned device structure showed a great improvement compared with traditional pairing methods, the throughput is not very high due to the limitation in the micro-orifice integration, which is aligned in a linear manner

along the channel. This one-dimensional distribution is unsuitable for massive parallelism. To avoid this limitation, Kimura et al. [89] developed a new microfluidic device with micro-orifice array sheet. The cell pairing protocol is accomplished by the dielectrophoresis-assisted massively parallel cell pairing based on micro-orifice induced field constriction. The core of this new device is a 4 mm diameter and 25 μm thickness polyimide chip with 6×10^3 micro-orifices in two-dimensional arrangement (cf. Fig. 6a). The micro-orifices of 5–8 μm in diameter are arranged in triangular array with a pitch of 50 μm (cf. Fig. 6b). This polyimide chip, sandwiched between two indium tin oxide (ITO)-coated glass electrodes, and two PDMS sheet spacers of 200 μm thickness with a circular opening of 4 mm in diameter conform the microfluidic device. The cell pairing protocol can be divided into 3 steps (cf. Fig. 6c–e): firstly, adding cell suspension (low-conductivity medium: 150 $\mu\text{S}/\text{cm}$) of two types of cells into upper and lower chambers, respectively. Cells A (green cells, whose cytoplasm are stained with green fluorescence dye) in the upper chamber (Chamber A) start sedimentation and move to the micro-orifice under the positive DEP force produced by the applied 1 MHz AC voltage between the ITO electrodes (cf. Fig. 6c). Since the high electric field gradient only exists in the vicinity of the orifice, cells B cannot be lifted to the micro-orifice sheet from the lower chamber B by the DEP force. The microdevice needs to be flipped over keeping AC voltage 'ON' to keep cells A attached to the micro-orifice in chamber A by the DEP force (cf. Fig. 6d). By the gravity and the DEP force, cells B in the other chamber (Chamber B, which is now becomes upper chamber after flipping) start sedimentation toward the orifice to form cell pairs in the orifice. To avoid the cells B to keep in touch with the upper electrode, stirring bar is used to scrape them off. In addition, the stirring is helpful for pearl-chains disruption and homogeneous distribution of the cells in the orifices (cf. Fig. 6e). The cell pairing result shows that more than 80% of the orifices with this cell pairing process form AB cell pairs as reported by Kimura et al. [89]. However, both of these one-dimensional and two-dimensional arrangements of micro-orifice arrays in the

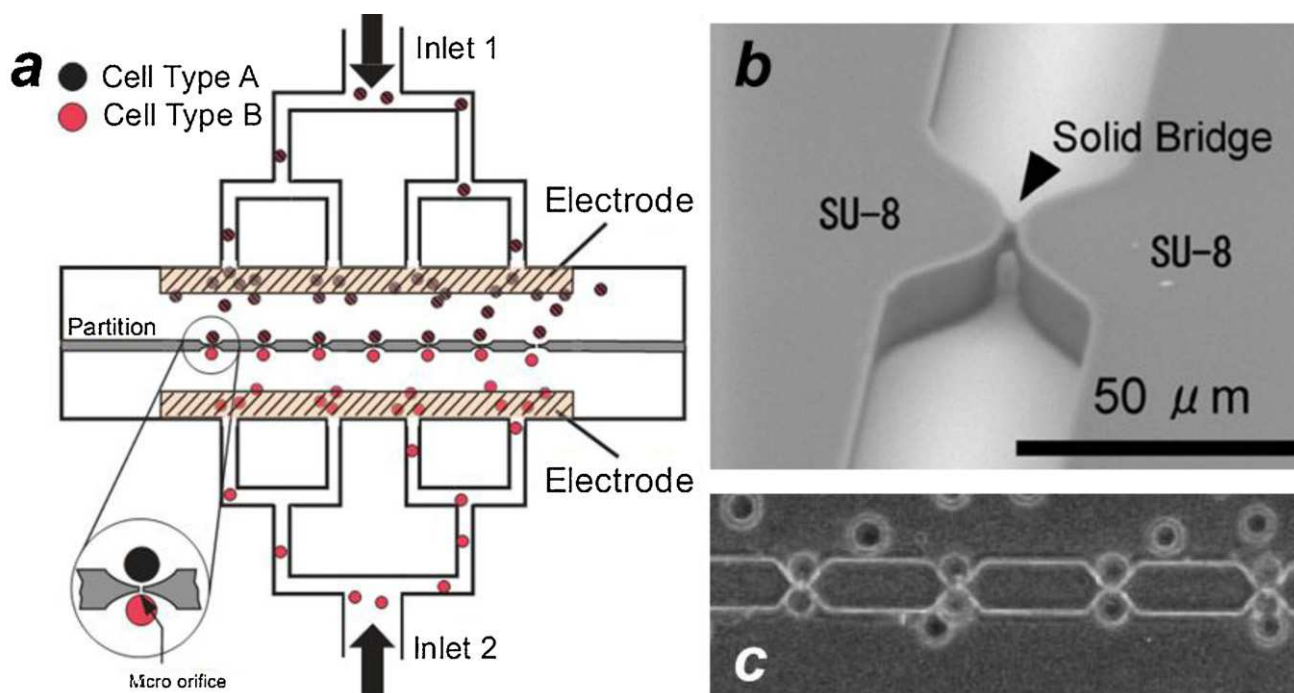


Fig. 5. Cell pairing process on microfluidic chip with 1D micro-orifice array. (a) Schematic of microfluidic chip and cell pairing process. Adapted with permission from Ref. [46]. (b) SEM micrograph showing the actual micro-orifice structure. Adapted with permission from Ref. [88]. (c) Optical microscopic view of cell pairing in the microchannel. Adapted with permission from Ref. [46].

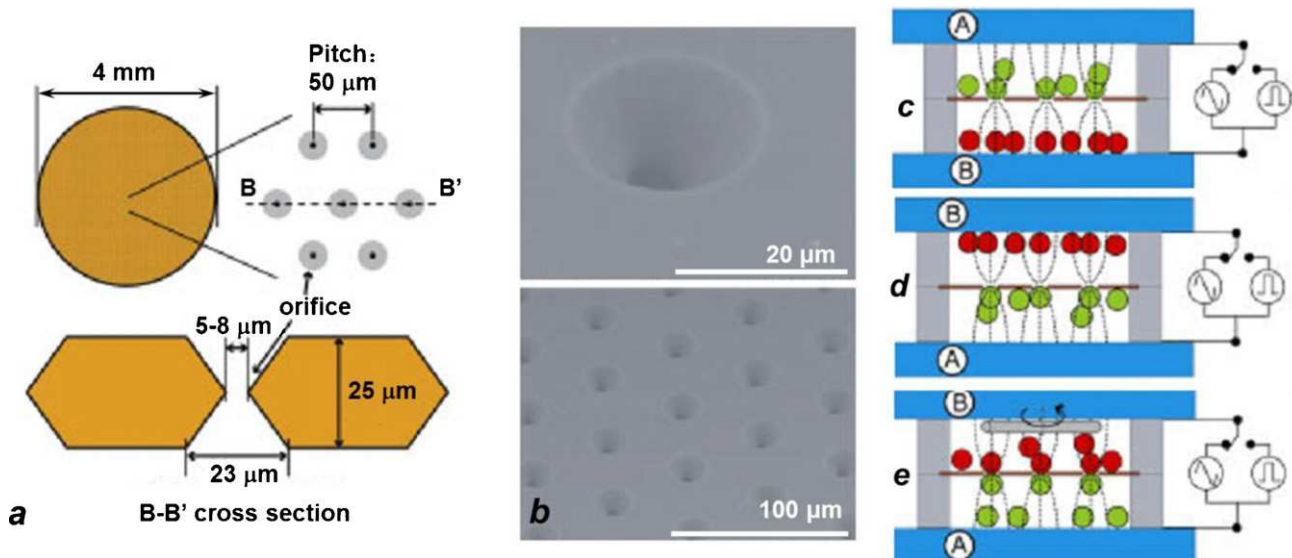


Fig. 6. Microfluidic device containing 2D micro-orifice array and resulting cell pairing process. (a) Schematic diagram of the micro-orifice structure and dimensions, (b) SEM images of a single and an array of micro-orifices. (c–e) Schematic procedure for cell pairing on the 2D orifice array. Adapted with permission from Ref. [89].

microfluidic devices need a complex operation, especially to control the intensity of the AC field to make sure that cell A can be trapped at the micro-orifice and avoid the cell damage by excessive dielectrophoretic force.

Compared with cells that are placed on each side of the micro-orifice construction, Clow et al. [73] developed a microfluidic device that was integrated with micropit structure for cell pairing by dielectrophoretic force. A schematic cross-sectional view of the micropit structure is shown in Fig. 7a. The design aimed to improve the cell pairing between the donor cells and the cytoplasts and automate the nuclear transfer procedure. This group used different micropit dimensions (larger, smaller or comparable to cell size, shown in Fig. 7b) to observe cell-pairing efficiency between cells having comparable or widely varied dimensions. In addition, this method eliminates the problem of cell settling or moving away from below the insulating film. On this microfluidic device, dielectrophoretic force was used to attract cells toward the micropit and automatically form couplets on the same side of the insulating film. For cell-pairing between two widely varied cells (such as oocyte and somatic cells), firstly, 1 MHz, 3 V_{rms} AC voltage was applied, which produced a dielectrophoretic force to attract somatic donor cells within ~50 μm of a micropit edge and become trapped. Numerical simulation shows that the DEP force is approximately zero as the field is essentially uniform in this region over 250 μm. It means that cells in this area cannot be driven by the DEP force. In addition, higher voltage (above 8 V_{rms}) is forbidden to avoid consistent cell lysis. After the first donor cell positioned itself centrally within a pit, the oocyte (having much larger diameter than donor cells) was dispensed and migrated to the pit. The final location of the oocyte was vertically above the donor cell. A couplet was formed between the first donor cell and the oocyte (cf. Fig. 7c). For cell pairing between two cells having comparable dimension (such as oocyte–oocyte pairing, shown in Fig. 7d), the first oocyte particle was also attracted, and located over the pit by the DEP force. Since the diameter of the oocyte is bigger than the size of the micropit, it was positioned directly over the pit. Then the second oocyte was released near the edge of the titanium film electrode, and allowed to drift until it made contact and formed the couplet with the first oocyte. The limitation of this microfluidic device is the adoption of wide variations in the cell and the micropit size. For larger micropit, there is a probability of two or more donor cells to be trapped in the same micropit, and then these donor cells can contact and fuse

with the subsequently loaded oocyte to form one-oocyte-multi-donor-cells. In order to overcome this problem a separation method based on cell size has been adopted by various groups [90–92] with micropit-based microfluidic devices. Based on pit diameter, size pre-selection of somatic donor cells resulted in an average cell diameter around 20 μm in the fusion buffer. However, this method can be elaborate and costly.

2.3. Cell pairing by microstructure

Cell pairing just by microfluidic control also attracts high attention in recent years. This method always integrates micro-trap structure on microfluidic chip. Cell pairing then is accomplished by flow control and cell trapping in the micro-trap structure.

Recently, Skelley et al. [93] developed 2-cell capture and pairing method on a microfluidic chip, which showed great potential in high-throughput and high-efficiency cell fusion of two types of cells. This capture protocol is based on trap structure with larger front-side and smaller backside capture cups. The details of the trap structure, including the larger front-side and smaller backside capture cups (14 μm tall, 18 μm wide × 25–40 μm deep and 10 μm wide × 5 mm deep, respectively), along with support pillars (7.5 μm wide × 35–50 μm long × 6–8 μm tall) are shown in Fig. 8a. The chip is integrated with 6000 traps on 8 mm × 4 mm array. The loading protocol can be divided into three steps: firstly, one type of cell (green cell) was loaded into the microfluidic chip. These cells were isolated in the smaller backside capture cups with the hydrodynamic pressure until the array was saturated. Since the size of the backside capture cup is very small, just one green cell can be captured there. Secondly, the green cells on the smaller cups were transferred directly 'down' into the larger capture cups, placed just opposite to it, under an inverted laminar flow. And this laminar flow within the device can ensure the transfer process to be fast, massively parallel and highly efficient. Finally, another type of cell (red cell) was loaded into microfluidic device. Under the hydrodynamic pressure, these cells would be trapped in front of the previously trapped cells within the larger capture cups. Since the larger cups were designed to capture only 2 cells, additional cells cannot enter the cup, and traveled through the array to another cup until the array is saturated (cf. Fig. 8b–d). On this microfluidic device, 2-cell capture and pairing efficiencies are up to ~80% and 70%, respectively. This method can control thousands of cell pairing

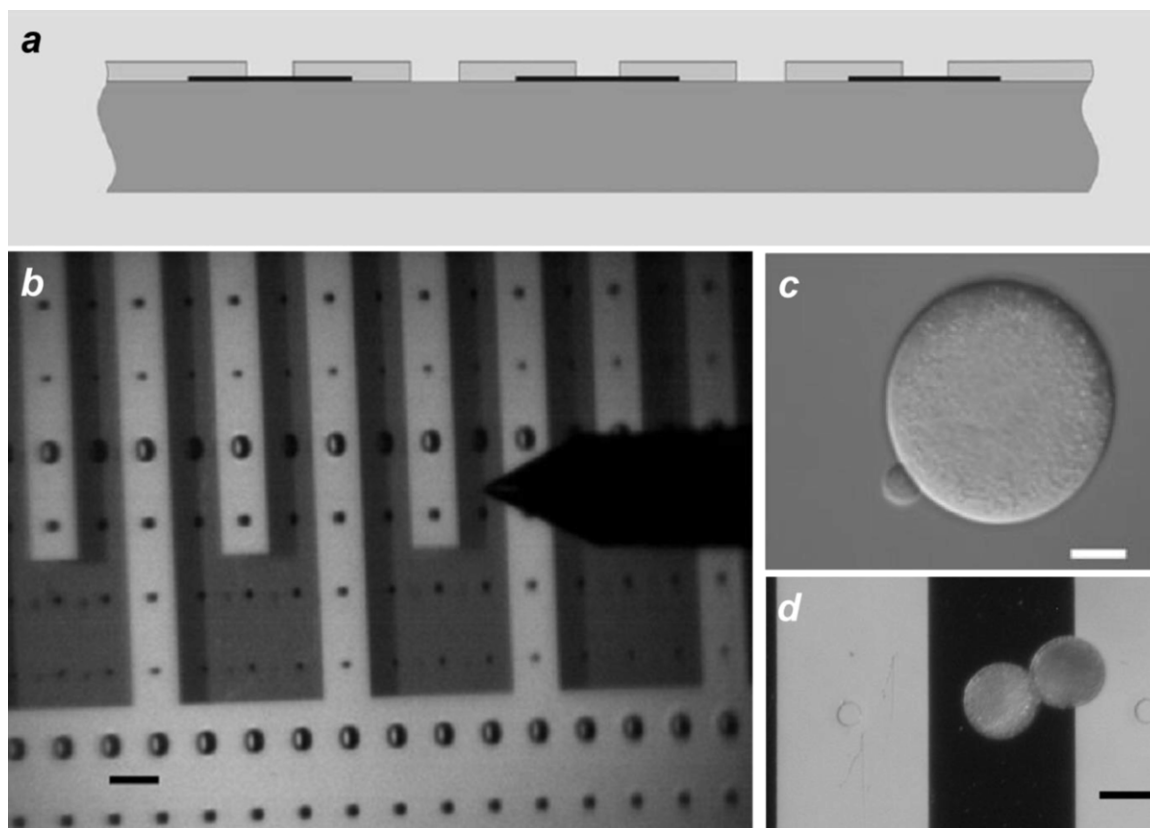


Fig. 7. Cell pairing on the microfluidic chip with micropit. (a) A schematic cross-sectional view of the micropit structure, showing Titanium micro-electrodes (black), borosilicate glass substrate (grey) and, SU8 (light grey, not to the scale). (b) Image of the actual microfluidic chip containing an array of 22 μm deep pits (pyrex substrate/grey, and titanium film electrodes/light grey). (c) Donor-oocytes cell pairing. (d) Pairing of Oocytes located on a 40 μm pit (titanium electrodes/black). Scale bars of b, c and d are 250, 100, 30 μm , respectively. Adapted with permission from Ref. [73].

in a short time. In addition, the throughput of this device can be increased by increasing the size of the substrate and by integrating more capture microstructures on this microfluidic chip. Also the cell pairing efficiency is found to be higher than the existing microfluidic devices. In this cell pairing protocol, the most important factor is that the backside traps just accommodate one A cell due to its small size. It ensures that in the next front side capture *via* 'transfer down' process, just one A cell can be trapped. However, the pairing of two B cells as well as multi-cell pairing cannot be avoided in this method as depicted by the white circle in the microscopic image of Fig. 8d. Moreover, this method also needs modification for the adoption of cell-pairing between two types of cell with significantly different in diameter, such as oocyte and somatic cells. The size of the front capture microstructure should be adopted according to the size of cells to make sure that the cell can be trapped into it. Finally, significant attention to be paid to minimize the frictional force on cell membrane and its potential damage on cells during the cell pairing process.

As with the micro-capture structure, another microfluidic chip with trap array was developed by Kemna et al. [94], for hybridomas generation between human peripheral blood B-cells and mouse myeloma (NS-1) cells by electrofusion. 11 rows of 87 traps were integrated on the microfluidic chip for high throughput electrofusion (*cf.* Fig. 9a). The space between two rows was 50 μm , and the distance between the traps was varied. Each trap structure was composed of a V-shaped trap (width: 25–29 μm ; length: 20–21 μm) with a small trap (depth: 3 or 6 μm) placed at the center of the large trap (Fig. 9b). Firstly, the isolated B cells (having smaller diameter) were loaded into the device by using a syringe

pump. After B cells trapped on the smaller traps, the cell suspension with NS-1 cells (having larger diameter) was loaded into the device. Under the pressure-driven flow, NS-1 cells were trapped in the large trap structures and form B cell/NS-1 cell pairs (*cf.* Fig. 9c). The cell pairing result shows that the small trap with 6 μm depth has better performance in trapping B cells (trapping efficiency is $77 \pm 2.3\%$), compared with small trap with 3 μm depth (trapping efficiency is $42 \pm 20\%$), as the 3 μm trap is too small to trap B cells. The distance between two adjacent traps (d_t) on the same row also has significant influence on the capture of NS-1 cells. The highest trapping efficiency ($83 \pm 3.5\%$) occurred at $d_t = 25 \mu\text{m}$. In contrast, the trapping efficiencies for $d_t = 20$ or 30 μm are $56 \pm 6.5\%$ and $71 \pm 2.5\%$, respectively. And excessively narrow gaps between two traps ($d_t = 20 \mu\text{m}$) resulted in clogging of the device. In addition, the width of small trap is another important factor affecting the cell pairing efficiency. The pairing efficiency (the percentage of traps occupied by exactly one B-cell and one NS-1 cell) is $33 \pm 6.4\%$, $31 \pm 9.3\%$, and $19 \pm 4.9\%$, respectively, as the widths of the small traps varied as 4, 5, 6 μm , respectively. This study reveals that this microstructure has great potential application in high efficiency heterogeneous cell pairing. Some novel designing modification of this device can pair two types of cells with different diameters. It has been observed that the ratio between cell diameter and separation between traps affects the trapping efficiency and pairing efficiency significantly. Therefore the sizes of the cells as well as the trap structure should be chosen carefully in this type of microfluidic device for efficient cell electrofusion. In addition, the variation in the cell diameter may add complexity into the device operation. Some microstructures with more adaptability are

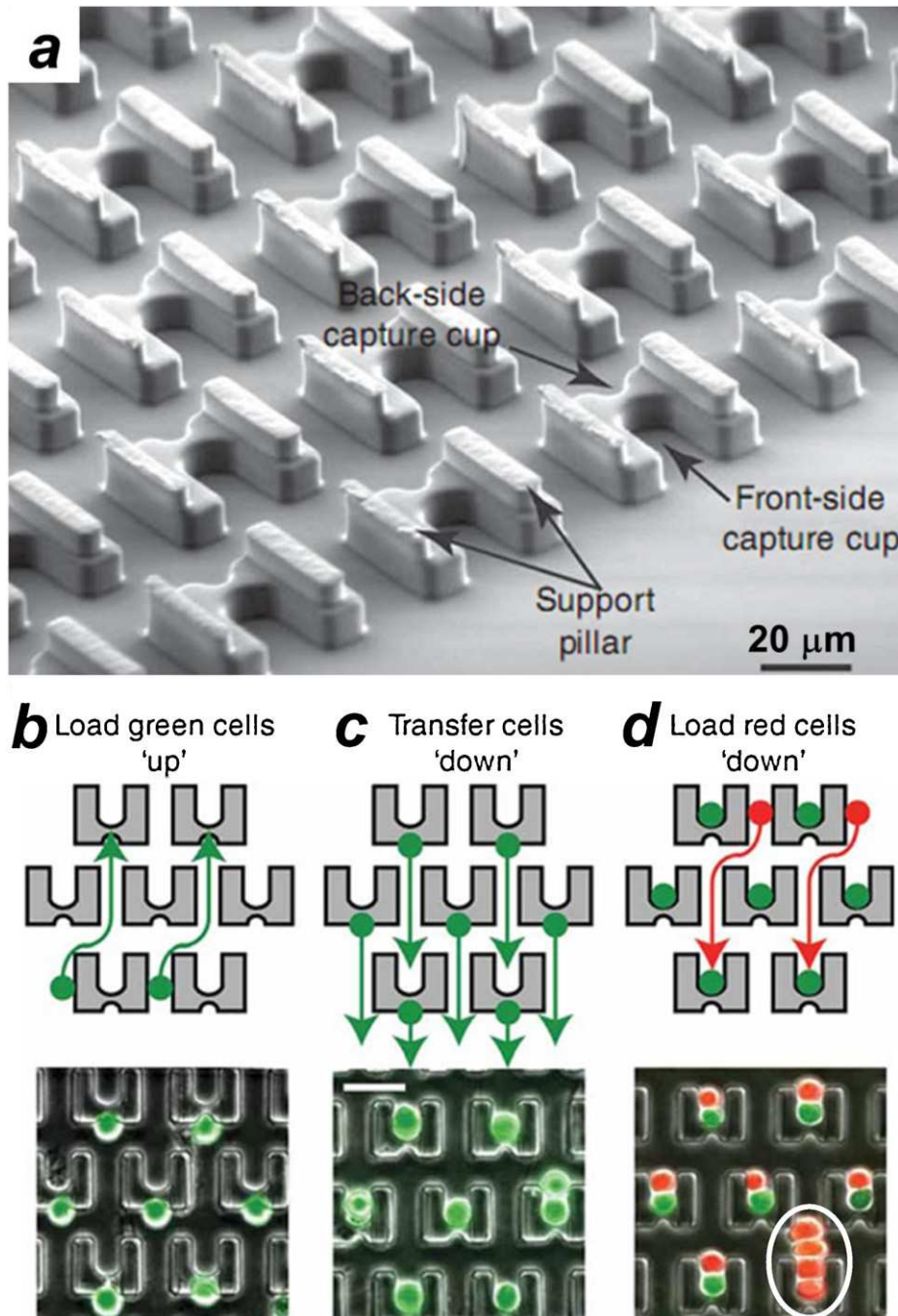


Fig. 8. Images of an array of micro trap structures and cell pairing processes on the microfluidic device. (a) picture of the actual trap structure, including the larger front-side and smaller back-side capture cups. (b–d). Three-step cell-loading protocol. (b) Cells are first loaded 'up' toward the smaller back-side capture cup. (c) The direction of the flow is reversed, and the cells are transferred 'down' into the larger front-side capture cup two rows below. (d) The second cell type is loaded from the top, and cells are captured in front of the first cell type. Adapted with permission from Ref. [93].

desirable to obtain high efficiency for heterogeneous cell pairing between two types of cells with different diameters.

To summarize, it has been clearly depicted that the cell pairing efficiency, especially heterogeneous cell pairing, is one of the most important parameters for evaluating the performance of cell electrofusion process. In the aforementioned microfluidic devices, the cell pairing is carried out by chemical, electric field, or field-free microstructure-assisted microfluidic trapping. Dielectrophoretic force, hydromantic force, gravity force and chemical conjugation are used in these processes, and show great potential to improve the cell pairing efficiency. The advantage of electric field-assisted cell

pairing is that it is easy to operate and has widespread applications. Electric field induced by microelectrodes can realize cell pairing without size limitation. Optimized microelectrode structure, like discrete microelectrodes and thin-film electrodes can improve the one-to-one cell pairing efficiency. However, this method cannot ensure heterogeneous cell pairing due to the random cell contact. On the other hand, electric field induced by constriction is better to conduct high efficiency of heterogeneous cell pairing. But it needs to resolve some issues, such as nucleus fusion and size-adoption. The chemical method shows good adoption of different types of cells due to pre-modification of each type of cell before cell pairing.

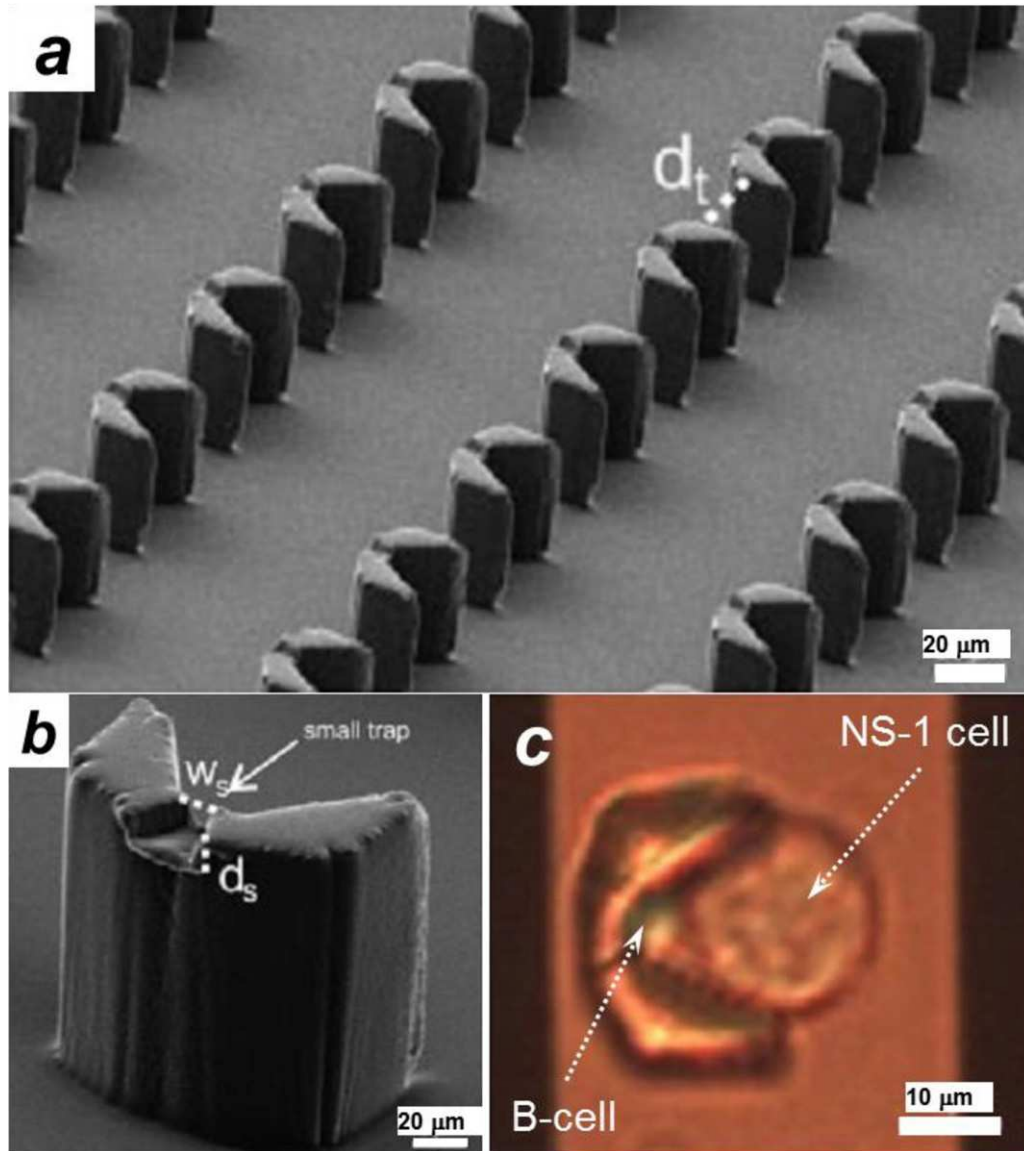


Fig. 9. Microfluidic device for cell capture by micro trap structure. (a) SEM image of the trap array, d_t represents the distance between the traps. (b) Detailed zoom of one trap structure, highlighting the large and small traps; w_s and d_s represent the width and depth of the small trap. (c) Cell pairing result between a CFDA stained B-cell and an unstained NS-1 cell. Adapted with permission from Ref. [94].

Table 1
Comparison between various cell pairing methods used in microfluidic devices.

Methods		Mechanism	Advantages	Disadvantages	References
Electric field-assisted	Field modification/enhancement by microelectrode geometry	Non-uniform electric field produced by microelectrodes	Easy to fabricate, Better adoptability of cell types	Low-heterogeneous cell pairing efficiency due to the random cell–cell contact	[74–77,79–83]
	Field modification/enhancement by microstructure between electrodes	Electric constriction by the micro-orifice/micro-holes	Improve the heterogeneous cell pairing efficiency	Cell size adoption is not good Nucleus fusion limitation	[46,73,87–89]
Field-free Microstructure-assisted		Cell trapping due to the flow/Microfluidic control	Improve the heterogeneous cell pairing efficiency, High specific cell pairing control	Complex microfluidic controlling system, and cell size adoption is not good due to the limitation of microstructures	[93,94]
Chemically conjugated		Bio-chemical junction	High through-put cell pairing method	Low heterogeneous cell pairing efficiency due to random contact in cell pairing process Pre-chemical-treatment induces potential damage of cell membrane Cell sample without pre-modify can't be paired	[48,49]

It allows two types of cells with significantly different diameters to be paired by chemical conjunction. But considerable attention needs to be paid to prevent the potential damage of the cells in pre-modification treatment, and the one cell A pairs with two or more cell B in random pair process. Moreover, the pre-modification treatment is also a complex procedure. Microstructure-assisted conjugation can realize high heterogeneous cell pairing. But there are still some issues related to the size adoption between cell sample and microstructure, which needs to be resolved. Combination of obstacle/micro-capture structure and the multi-controlling ability, such as dielectrophoresis and hydromantic pressure is considered to solve this problem and create a high efficiency, widely adoptable heterogeneous cell pairing method. Table 1 compares the various means for cell pairing used in microfluidic cell electrofusion devices.

3. Cell reversible electroporation

Cell reversible electroporation is one of the most interesting influences of electric field on cell [95]. Generally, after cell pairing process, high-strength DC electric pulses are applied *via* opposing electrodes (within the microfluidic platform), which are amplified at the cell membrane owing to the low conductance of the membrane. This leads to molecular rearrangement of the phospholipids [96], resulting in the formation of nanopores (and hence called 'electroporation'). And the nanopores of two cells in contact will

induce membrane connection, cytoplasm exchange, and eventually whole cell electrofusion process between the two paired cells. Obviously, application of excessive electric field will induce cell rupture, which needs to be avoided in cell electrofusion. Generation of highly concentrated electric field, strong enough for reversible electroporation (but not enough for cell rupture), can be achieved either by reducing the distance between the two electrodes or by constructing some microstructures, such as micro-orifice or micro-traps, that concentrate the electric field into a small region to provide the required electric field for cell reversible electroporation.

3.1. Cell reversible electroporation induced by microelectrodes

In the first approach, the electrodes are placed 20–100 μm apart, and cells were loaded in the microfluidic channel between two opposite microelectrodes. The electrofusion voltage is always under 50 V. In the research of Masuda et al. [86], the electroporation was accomplished by using 0–30 V, 20–100 μs single-shot pulse source by shortening the distance between the two electrodes and constricting the electric field. It eliminates the requirement of costly power source, and expands the application of cell electrofusion technology.

Later, various groups also developed different microfluidic devices integrated with the protruding microelectrode structure to induce low-voltage electroporation (<50 V) [48,74–76,78–83,97],

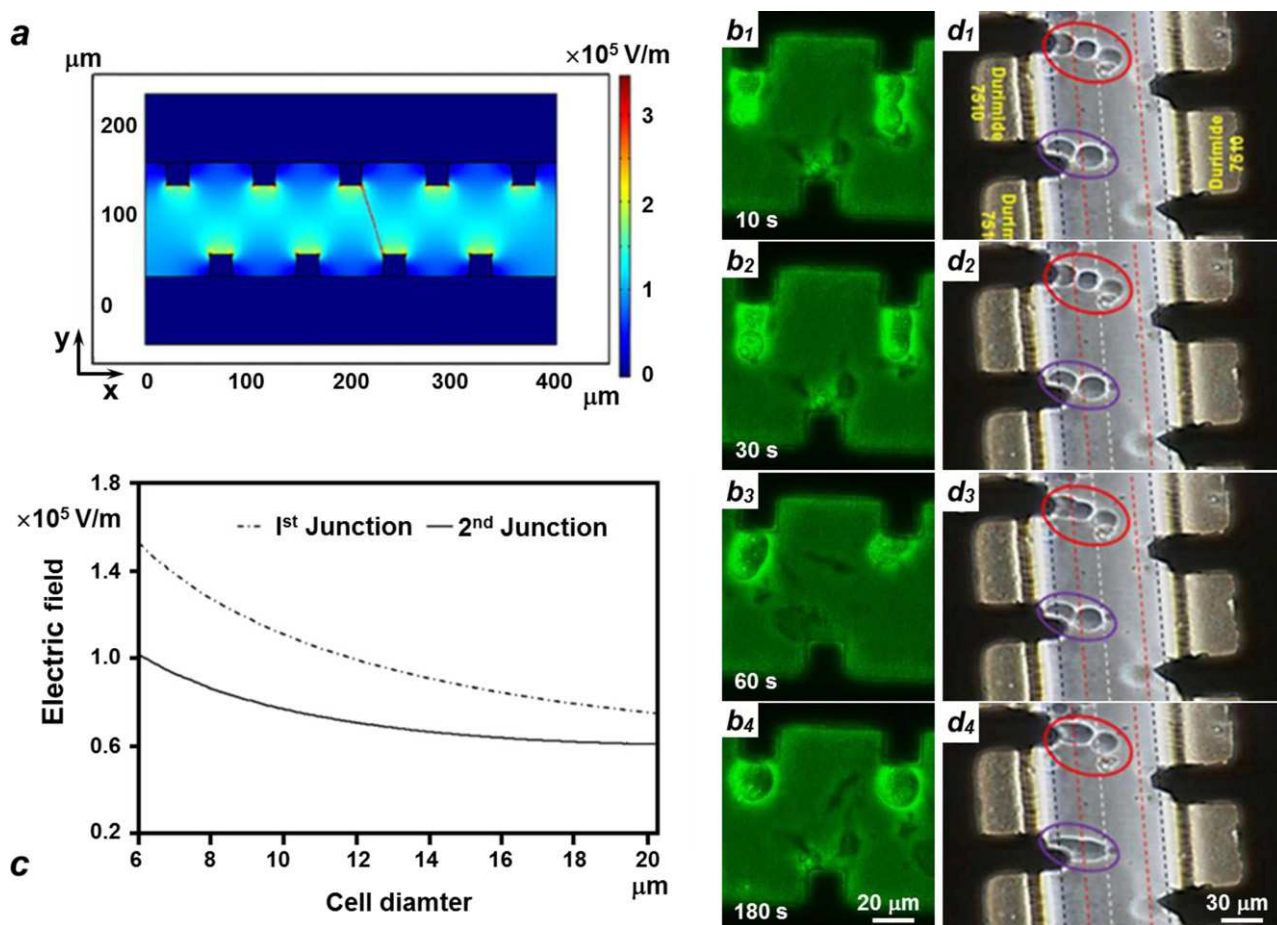


Fig. 10. Cell fusion between protruding microelectrode. (a) Electric field distribution in microfluidic chip based on glass-silicon bonding wafer. Adapted with permission from Ref. [83]. (b) The progression of cell fusion after the alignment of HEK293 cells is shown in a series of micrographs (b₁–b₄). (c) The predicted y-component electric field at the first (dash-dotted line) and second (solid line) cell junctions as a function of the cell-diameter. (d) Experimental observations of K562 cell fusion process and the elimination of multi-cell fusion, the purple circles are cell electrofusion between cell pairs, while the red circle shows the electrofusion occurring only at the first cell junction. Adapted with permission from Ref. [75].

as shown in Fig. 10a and b. These protruding microelectrodes can generate spatially non-uniform electric field distribution in the microfluidic channel. In the numerical simulation of Cao and co-authors [98], it has been reported that the electric fields in the zone near the microelectrode of symmetrical and asymmetrical protruding microelectrode arrays and the protruding/plate microelectrode structure are, respectively, 2.4, 2.0, 3.0 times of that in the parallel plate microelectrode structure. In addition, these microfluidic chips with protruding microelectrode structure always use the induced non-uniform electric field to produce DEP force and attract cells to pair on the microelectrodes. The cell junction position is still located at the high electric field zone. The reversible electroporation can be achieved under lower voltage compared to the parallel microelectrode structure. However, in the protruding microelectrode structure, the fusion within the cavity area ('dead area') [75] between two adjacent microelectrodes is inefficient due to the low electric field distribution compared with that near the protruding portions of the microelectrode. Therefore, the cells trapped in these areas by the DEP force or hydrodynamic force cannot be fused because of the low field distribution in these areas. As mentioned in the previous sections, Hu et al. [75,82] solved this problem by filling the cavity area with insulating material or floating silicon, which avoids cell trapping in the cavity. Moreover, the discrete microelectrode also concentrates the electric field and reduces the fusion voltage. In that case, under a lower voltage (<10V) K562 and NIH3T3 cells are fused into hybrid cells with a higher efficiency (~40% of total cells loaded into the device) than previously reported with protruding microelectrode-based cell electrofusion chips. In addition, the electric field distribution shows that the electric field decreases as the distance from the edge of microelectrode increases. It means that the electric field in the first junction in a cell chain is higher than that at the second junction (cf. Fig. 10c and d), which reduces multi-cell electrofusion since the electric field at the second junction is not enough to fuse the second and third cells at the second junction.

Recently Wang and Lu [48] developed a continuous flow cell electrofusion protocol in a microfluidic chip. The cell couplets, after chemical conjugation based on biotin–streptavidin interaction, continuously flowed through the microfluidic channel with 5 converging-diverging sections (shown in Fig. 11a). DC electric pulses are imposed between the opposing electrodes, and electroporation of these couplets occurs when they flow through the throats of the converging-diverging sections, where the electric field is highest as shown in Fig. 11b. The parameters of the DC pulses, including pulse voltage, duration, and number, depend on the dimensions and number of the converging-diverging sections and the continuous flow velocity. Under a series of DC pulses (the field intensity is about 1200 V/cm) in the throat, the couplets were reversibly electroporated and fused in a short time, as shown in Fig. 11c, with the highest efficiency of 44%. The throughput of this device is considerably high due to the use of continuous flow. The limitation of this microfluidic chip is that the fusion voltage is a little higher than that in the previous microfluidic chips. In addition, the flow velocity needs to be specifically controlled so that the couplets slowly translocate through the throats of the converging-diverging sections, where fusion occurs. Finally, cell pairing and fusion could not achieve in the same device, and cells must be paired by chemical method prior to being pumped into the device.

3.2. Cell reversible electroporation induced by electric field constriction

In the other approach of cell electroporation, the required electric field, necessary for electroporation, can be produced on the microfluidic chip with optimized microstructures under a low voltage, even if the distance between two opposite electrodes is

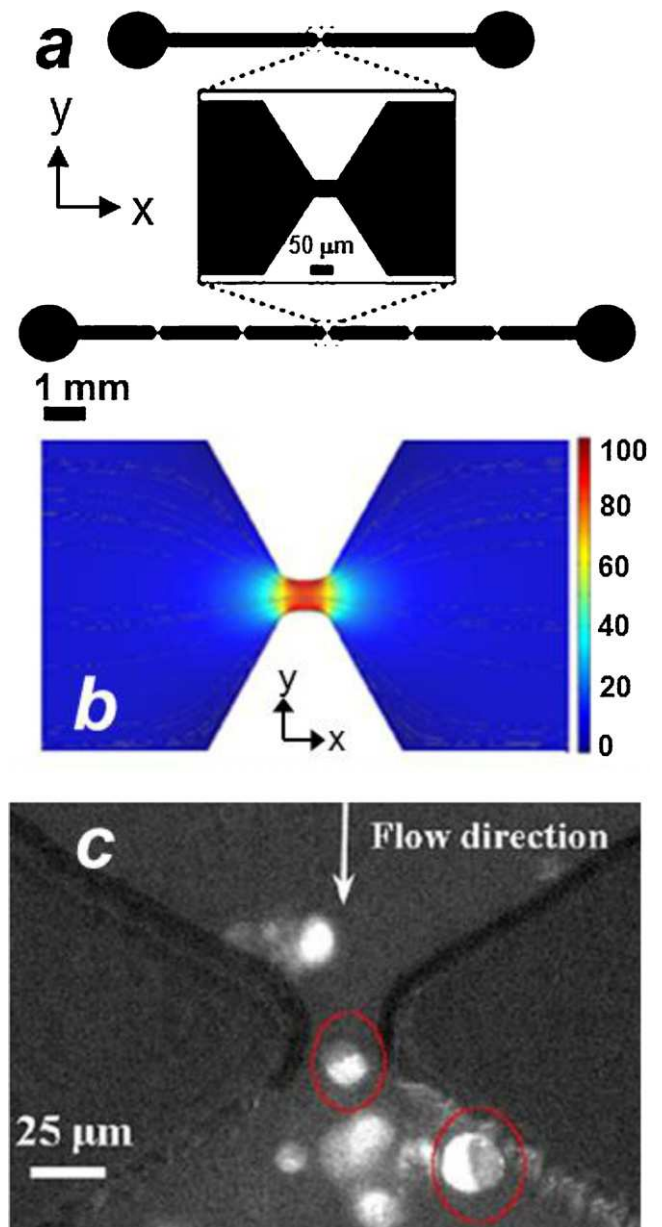


Fig. 11. Continuous electrofusion on microfluidic chip. (a) The schematic diagram of microfluidic chip with 5 narrow gaps for continuous microfluidic. (b) Electric field intensity simulation of micro-fluidic structure with alternating wide and narrow sections. (c) Image of the continuous electrofusion on microfluidic chip. Adapted with permission from Ref. [48].

relatively longer. These methods include either the development of micro-orifice structure or micro-traps to concentrate the electric field within a small region for efficient electroporation.

The Washizu group [46,86–89,99–101] developed a micro-orifice structure to concentrate the electric field distribution and reduce the fusion voltage. The device structure has already been described in previous sections related to the improved cell-pairing processes. The same construction shows the improved electroporation between cell pairs as well, indicating the importance and novelty of the micro-orifice structures. As reported by Shirakashi et al. [99], the membrane potential distribution simulated in the GUV-Jurkat cell contact point is higher than the top and end of the cell pair. However, there is similar membrane potential distribution at each cell–cell contact point within a long cell chain [102]. It is likely to produce undesirable multi-cell electrofusion.

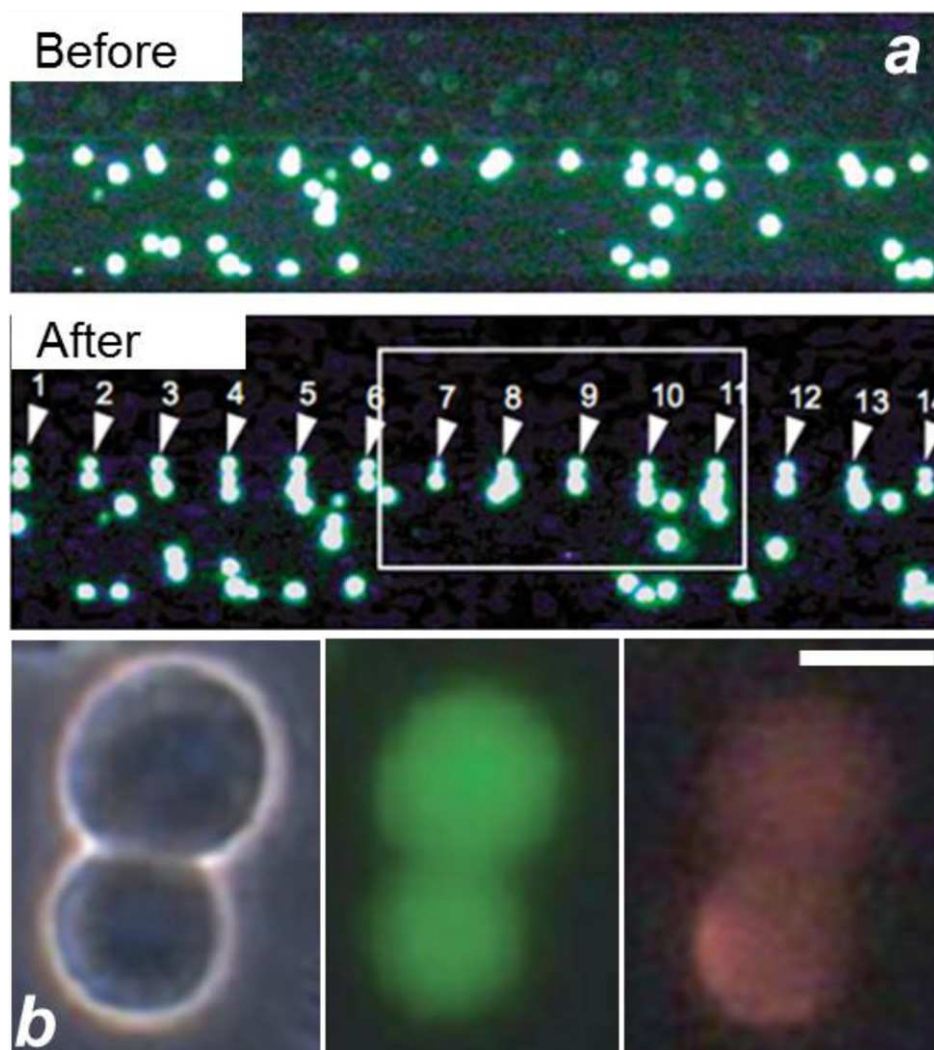


Fig. 12. Cell electrofusion process on microfluidic device with micro-orifice. (a) Fluorescent image of cells before fusion pulse and after fusion pulse, respectively. Adapted with permission from Ref. [46]. (b) Hybrid cell expressing green and red fluorescence after cell electrofusion (scale bar = 10 μm). Adapted with permission from Ref. [89].

The new microfluidic device, developed by the Washizu group, tries to address this issue by constructing an insulating wall with micro-orifices, whose size is comparable to cell size, along with two opposite electrodes on each side. When the electric signal was applied on the electrodes, the field lines were converged into the micro-orifices, yielding the highest electric field at the center of each micro-orifice. After two cells, paired at the micro-orifice due to DEP, the applied DC pulses induce the largest membrane voltage at the contact point for electroporation. The electrofusion sequence in this study composes of application of an AC field (10 V_{p-p}, 1 MHz) and then superposing a DC pulse (4 V, 300 μs) to the AC field and finally, application of AC field only for another 10 s. A neck between two cells is created and fluorescent dye was transferred from one cell to another (*cf.* Fig. 12). The fusion efficiency is found to be more than 95%, which is much higher than other microfluidic devices. In addition, this electric field distribution eliminates the multi-cell electrofusion and cell rupture, as the membrane voltages in other positions (such as the other cell contact points and both ends of cell chain), is lower than that at the contact point through the micro-orifice. However, since the size of the micro-orifice will affect the electrofusion performance, micro-orifice should be designed and fabricated according to the size of the cell sample. The size of the micro-orifice will influence the nucleus and the cytoplasmic contents' exchange. Under the pressure difference, which can be

induced by the flow control, the cytoplasmic contents of the cells will begin to move from one cell to another. In contrast, the nucleus cannot pass through the micro-orifice when its size is too small ($\sim 3 \mu\text{m}$). In that scenario, two parent cells will create two daughter cells without nucleus fusion (shown in Fig. 13). When the size of micro-orifice is larger than 5 μm , the nucleus could pass through the orifice and form a hybrid cell with two nuclei [88].

To enhance the throughput of this microfluidic device, two-dimensional micro-orifice array, based on polyimide film, is developed by Kimura et al. [89]. This is because of the fact that the one-dimensional distribution cannot integrate many micro-orifice structures. Based on the good cell pairing performance (one-to-one cell-pairs are formed in about 90% of the orifices), various sizes and types of cells (Jurkat, L929, K562/HL60) are fused with 78–90% fusion yield on this microfluidic device (*cf.* Fig. 12b). Moreover, this microfluidic device shows great potential for high-yield fusion of $\sim 4 \times 10^4$ cells on a centimeter-sized chip. And it can be developed as a powerful tool for creating genetic hybrids and epigenetic studies for regenerative medicine.

Another microfluidic chip, with microstructures containing a large trap in one side and a small trap at the other side is developed to efficiently fuse two types of cells with different sizes, for example, human CD19⁺ B cells (isoosmolar buffer condition: $7.5 \pm 1.2 \mu\text{m}$) with mouse myeloma cells (isoosmolar buffer

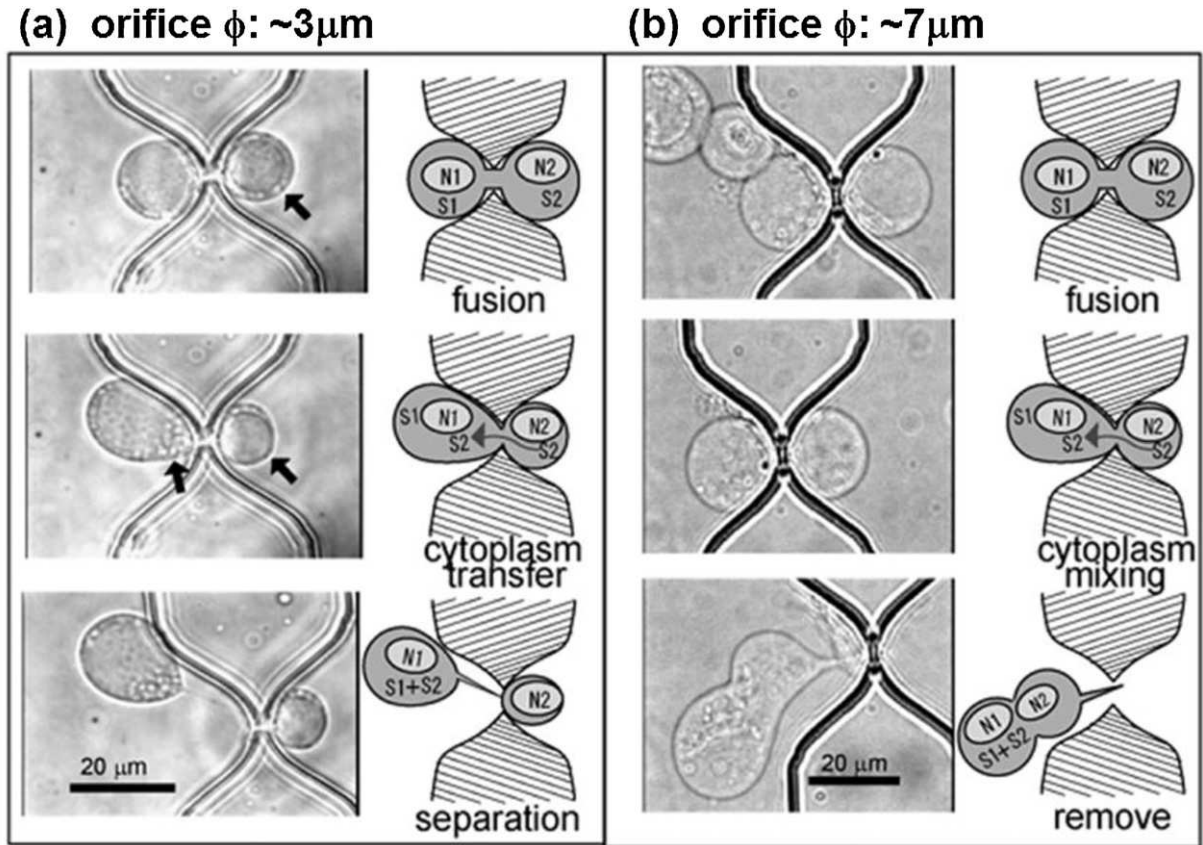


Fig. 13. Manipulation of the fusant with microfluidics. (a) Orifice size: 3 μm . (b) Orifice size 7 μm . Adapted with permission from Ref. [88].

condition: $15 \pm 1.8 \mu\text{m}$), to generate hybridomas. These hybridomas are able to produce human antibodies, which can be used for therapeutic applications. The cross-sectional view between the large and small traps, shows very high electric field constriction (as shown in Fig. 14a [94]), which manifest the efficient

electroporation between two types of cells. After pairing of the B cell and NS-1 cell, two distinct membranes were visible and the fluorescent dye CFDA was still localized in the B-cell (cf. Fig. 14b, $t=0 \text{ min}$). By applying six DC pulses (10 V, 100 μs pulse duration) with AC signal (2 V, 2 MHz and 30 s), the green NS-1 cells were

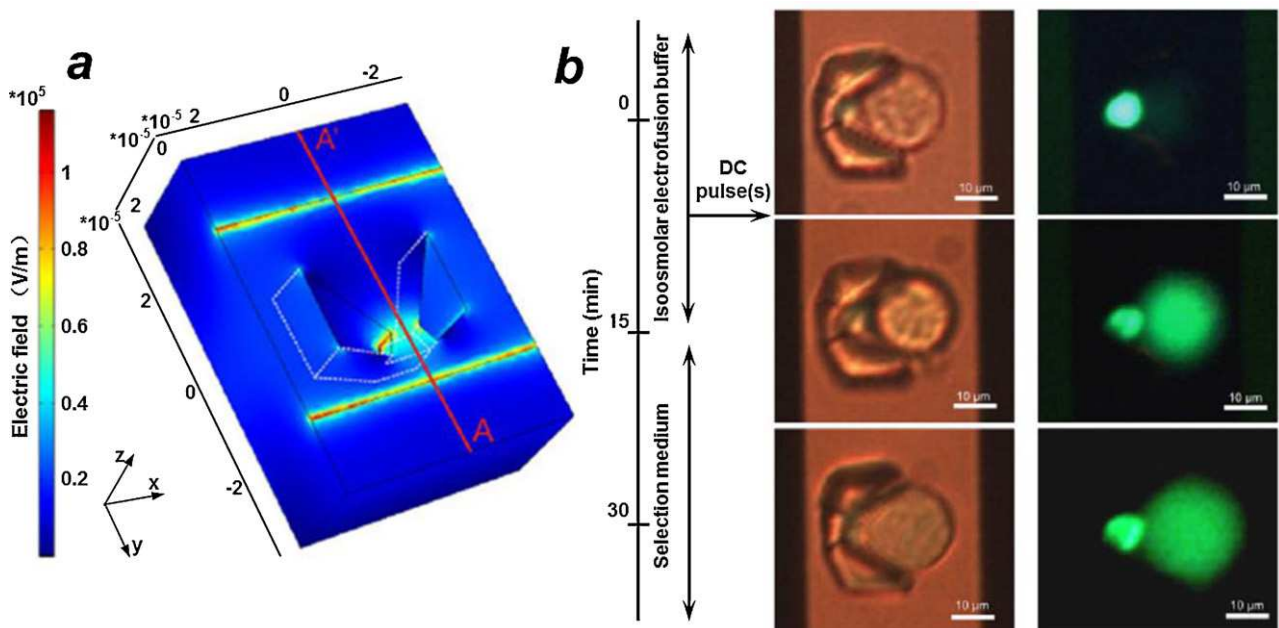


Fig. 14. Cell electrofusion process of B-cell and NS-1 cell. (a) The electric field distribution of single micro-trap. (b) Temporal sequence of electrofusion between a CFDA stained B-cell and an unstained NS-1 cell on microfluidic chip with micro-trap (contains small trap and large trap). Bright field (left) and fluorescent (right) images at ($t=0 \text{ min}$), $t=15 \text{ min}$ and $t=30 \text{ min}$ after applying 3 DC pulses of 50 μs with AC. Adapted with permission from Ref. [94].

observed, indicating that the cytosols of the two cells had connected and fusion was initiated (*cf.* Fig. 14b, $t = 15$ min). After 30 min, two cells form a hybridoma cell (*cf.* Fig. 14b, $t = 30$ min). The electrofusion efficiency of pronase-treated NS-1 cells and B cells is $51 \pm 11\%$, which is comparable or even higher than previously reported fusion yields of other cell types in microfluidic chips. Viable hybridomas were observed after 14 days of culture in hybridoma-specific medium, which is only suitable for hybridomas to survive. Viable hybridomas yield is 0.33% (six DC pulses of $50 \mu\text{s}$ with AC field {2 V, 2 MHz and 30 s} and no pronase treatment) or 1.2% (six DC pulses of $100 \mu\text{s}$ with AC field {2 V, 2 MHz and 30 s} and without pronase treatment), which is higher than the yields reported in the literature (for example, viable hybridomas yield of conventional bulk electrofusion is in the range of 0.001% [103,104]).

Besides DC pulses signal, DEP field induced by π -shifted radio-frequency (600 kHz, $1.9 V_{pp}$) in an eight-electrodes-cage is also used in cell electroporation. At the beginning of electroporation, cell-pair between a Myeloma cell and a B cell blast is trapped in the central area of the DEP field cage. After applying PORE/FUSE signal (12 kHz, $8 V_{pp}$), the highest membrane potential is created at the contact area of two cells. This electric field distribution avoids the cell rupture at the top or bottom areas on the cell pair. On this microfluidic device, cell electrofusion efficiency of two homologous B or myeloma cell pairs is 100% and 52%, respectively. In contrast, the heterologous cell fusion efficiency is just about 37%. This lower fusion yield is probably due to the inconsistent composition of membrane [71].

In summary, electric field induced by microelectrodes and microstructure can reduce the operating voltage for reversible electroporation. It is helpful to create a low-cost electrofusion method. Moreover, the microelectrodes or the microstructures for electric field constriction provide optimized electric field distribution, which improves the electrofusion efficiency. Especially the electric field constriction produces highly localized strong electric field at the contact point between two desirable cells, and thus, it eliminates the multi-cell fusion and membrane rupture at both ends of cell chains. Finally, the throughput of these microfluidic devices can be increased by integration of a great number of microelectrodes or microstructures. Table 2 compares various methods used for cell reversible electroporation in microfluidics.

4. Other important factors affecting the performance of cell electrofusion

4.1. Geometry and material of microelectrodes

In a conventional electrofusion system, the cell electrofusion is performed between two parallel-plate electrodes. The electric field is therefore uniform in the fusion chamber, which creates several disadvantages, including multi-cell fusion, high joule heating, and low controllability. To overcome these problems, protruding microelectrode [74,76,79–81,83] was integrated within the microfluidic chips, as mentioned earlier. This microelectrode can concentrate the electric field in the region near the edge of the protruding portion of the microelectrode and produce a non-uniform electric field distribution. The advantage of this distribution is that the reversible electroporation can be induced by a lower voltage compared to the voltage produced in the parallel electrode system with similar electrode-gap. It means that one can control the electric field intensity only in the region near the edges of the protruding portions of the microelectrode above the reversible electroporation threshold, while the electric fields in most of the other places are kept at a lower intensity, which actually reduces the Joule heating to a considerable extent. Furthermore, the rapid decay of the

electric field, away from the edges of the protruding electrodes, ensures that the electric field strength at far side of the cell chain is not sufficient enough for multi-cell electrofusion.

In the protruding microelectrode system, the electric field lines (generated between two opposite sidewalls of two adjacent microelectrodes, which is basically the fusion region) are, on an average, parallel to the substrate, except the fringing fields near the electrode edges where some non-uniformity is created due to the electrode geometry, which enhances the cell-pairing, as discussed in the previous sections. Recently, application of electric field gradient along the vertical direction (*i.e.* perpendicular to the substrate) has also attracted much attention, as it affects considerably the electrofusion performance. In this regard, coplanar thin film electrodes, patterned on the substrate by gold or similar noble metals, are widely used in microfluidic devices [105,106]. Because of the significantly smaller thickness (~ 100 nm) of the electrodes, the electric field lines are concentrated more at the edges of the thin film electrodes (due to very high surface charge density at the edges), and drop significantly away from the edges. Therefore, close to the electrodes the equipotential surfaces bend asymptotically towards the substrates creating a vertical component of the applied electric field [48]. This enhances the cell pairing near the edges of the thin film electrodes. Away from the edges, the electric field strength drops very quickly and only at the halfway between two adjacent thin-film electrodes (which is the fusion region), the electric field becomes relatively uniform (*i.e.* the equipotential surfaces become nearly vertical to the substrate). Due to this rapid decay of the field strength away from the edges of the thin film electrodes, the electric field may not be enough for membrane disruption to occur at the contact point of the paired cells in the fusion region. This issue can be resolved or minimized by keeping the distance between the two co-planer electrodes at a much larger value than the cell size. In that scenario, the non-uniformity of the electric field within the fusion region becomes lesser and the application of a suitable voltage between the coplanar thin film electrodes manifests the cell-electrofusion. However, a larger distance between the co-planner thin film electrodes generally leads to the application of higher voltage, which is energetically not favored for this type of microfluidic applications. On the contrary, for protruding microelectrode system, which is having much higher thickness (or height, which is comparable to the cell size ~ 30 – $40 \mu\text{m}$), the electric field within the fusion region (*i.e.* the intermediate region between the two parallel side-walls of the electrodes) is found to be considerably uniform compared to the coplanar thin film electrode system (having identical potential difference). Indeed, a recent study by Clow et al. [49] showed that the applied voltage on thin film electrodes is $\pi/2$ times higher than that between two thicker electrodes to achieve equivalent field strength when the couplets are placed in the fusion region. Therefore, thicker electrode system attracts more attentions because of the fact that it reduces the working voltage and nullifies considerably the drawbacks in traditional electrofusion system, like Joule heating, bubble generation, extreme pH condition, and swelling of the cells. But the advantages of thin film electrode are that this kind of electrode can easily be fabricated by various thin film deposition techniques, such as evaporation, sputtering, electroplating, electrodeless deposition, mechanical lamination, conductive painting, or by using metallic adhesive tapes. Another very important advantage of the thin-film electrode is that it can be easily integrated with other photolithographic based devices. This capability allows the microfluidic electrofusion device to obtain the 'biochip' ability, like cell loading, cell separation, cell culture *etc.*, by integrating various micro-components like electro-hydrodynamic pumps, cell sorters, and microfluidic culture, among others. This type of integration can increase the throughput, reliability, and automation of the cell electrofusion process on the microfluidic device.

Table 2
Comparison of various methods for cell reversible electroporation in microfluidic devices.

Methods	Mechanism	Advantages	Disadvantages	Cell types	Fusion electrical parameters	Fusion efficiency	References
Microelectrode-assisted cell reversible electroporation	Using microelectrode to produce sufficient electric field under low power generator, by shortening the distance between two microelectrodes.	low working voltage; optimized non-uniform electric field can reduce the multi-cell electrofusion	Dead area in continuous protruding microelectrodes reduces the cell fusion efficiency Highest electric field near the microelectrode exists, which can manifest the potential cell rupture of the cells attached to the microelectrodes	CHO-K1 AESF-1(s), AESF-1, EFC(s), Oocyte, Cytoplasm RBC, liposome	600–1000 V/cm 110–160 V	28–42% 50–78%	[48] [49,73]
				Liposome, <i>E. coli</i>	DC pulse (2–3 kV cm ⁻¹ , 20 μs) 5–6 DC pulses (10 μs, 1–15 kV cm ⁻¹) 20 ms, 1.0 kV cm ⁻¹	- ~50–75%	[97] [74]
				Brassica campestris, Arabidopsis thaliana, Nicotiana tabacum, Peucedanum japonicum, Glehnia littoralis pigeon blood cells, HEK293, cucumber mesophyll protoplasts HEK293, NIH3T3, mESC	3–7 kV cm ⁻¹ , 20–50 μs, 3–9 pulses	3–5% 42 ± 2% of paired cells	[80] [81]
				HEK293, tobacco cytoplasm K562	10–20 V, 50 μs, 3–5 DC pulses 9 V, 50 μs, 3–5 DC pulses	46–60% of paired cells ~40%	[83] [79]
						43.1%	[75,82]
Electric field constriction-assisted cell reversible electroporation	By concentrating the electric field in microstructure.	Reduce working voltage by local electric field constriction; Reduce the multi-cell electrofusion due to the high electric field area just local at the connect point of desired cell pairs	Cell size adoption due to size limitation of microstructure for electric field concentration	Jurkat, L929, K562, HL60 L929	DC pulse (10 V, 50 ms)	78–90%	[89]
					4 V, 300 μs + 10 V _{rms} , 1 MHz 10 s	>95%	[46,88]
				NS-1, B-cell	6 DC pulses (100 μs, 2.5 kV cm ⁻¹) + AC field (30 s, 2 MHz, 500 V/cm)	51 ± 11% of paired cells	[94]

The materials of the electrodes also play an important role in cell electrofusion studies. The material of electrodes with good electrical and chemical stability can avoid producing some contaminations that may be harmful for the cell viability. This is because the electrodes are always kept directly in contact with the buffer solution. Therefore, the most important parameters to evaluate the material for the electrode are conductivity, fabrication feasibility, biocompatibility, and corrosion resistivity. Silicon is a common material for the fabrication of microchip. The advantage of silicon is that it is highly suitable for MEMS-based micro-fabrication techniques. Especially, silicon based microfluidic chip can be fabricated with high aspect sidewall microelectrode [79,82,107]. Moreover, the biocompatibility of silicon ensures that there is no toxicity to cell sample during the electrofusion procedure. However, one important disadvantage of Si is that its conductivity is not very good with respect to various other materials, especially for metallic electrodes. Therefore, for electrode arrays with very narrow width, the overall resistance of Si electrodes becomes poorer, which leads to inefficient performance of the electrofusion device. To overcome this problem, various groups attempted to use doped silicon to improve the conductivity. But still the improvement is not fully satisfactory, as Hu et al. [79] reported in the numerical model, which revealed that the peak electric field decreased by 9.5% along the microelectrode array made up of highly doped silicon. This indicates that the resistance of the doped silicon is still considerably higher and hence, creates a large potential drop across the electrode array. This variation in the electric field strength across the protruding microelectrode array actually translates into the variability of cell alignment and electrofusion, and could lower the overall cell electrofusion efficiency. To solve this problem, aluminum conductive films were added on the microfluidic chip to improve the electric field distribution around the protruding microelectrodes [79]. Also a very thin SiO₂ layer is deposited on the Al surface, as the biocompatibility of Al is not very good. Other metals with good conductivity have been tried as well by various groups. For example, Hu et al. [77] used copper as the electrode material for their protruding microelectrode system. However, the toxicity of released Cu²⁺ is deterrent for cell viability and therefore, this group modified the electrode structure by covering the copper electrode surface with Au film to prevent the reaction between the copper electrode and buffer solution. This Au film improves the biocompatibility and the corrosion resistivity of the microfluidic device because of the fact that Au is a very good biocompatible material, and therefore, considerably helpful to the survival rate of the hybrid cells. Besides the application in packaged copper electrodes, the Au material has also been used as thin-film discrete sidewall microelectrode [80] in the form of Ti/Au composite film for controlling the cell pairing and electrofusion.

4.2. Electronics signal

The performance of microfluidic chip also depends on the fusion signal. The fusion signal can be divided into 3 parts: AC signal for cell pairing, DC pulses for reversible electroporation, and post-fusion AC signal to keep close contact of cell pairs.

The main function of AC signal is to induce dielectrophoretic force and polarization of cells. Under the mutual attraction of polarized cells, cell pairing is realized. Recently Hu et al. [79] imposed an AC signal across the protruding microelectrodes used by Tresset and Takeuchi [74] to induce positive DEP force for cell pairing. In their report Hu and co-authors [79] performed the cell pairing of mesophyll protoplasts under variable AC voltages on a SOI-based microfluidic chip with protruding microelectrode array. The experiments revealed that the mesophyll protoplasts were aligned as cell pairs without cell deformation at $V_{p-p} = 4\text{ V}$. When $V_{p-p} = 6\text{ V}$, the membrane of the mesophyll protoplasts appeared to be deformed.

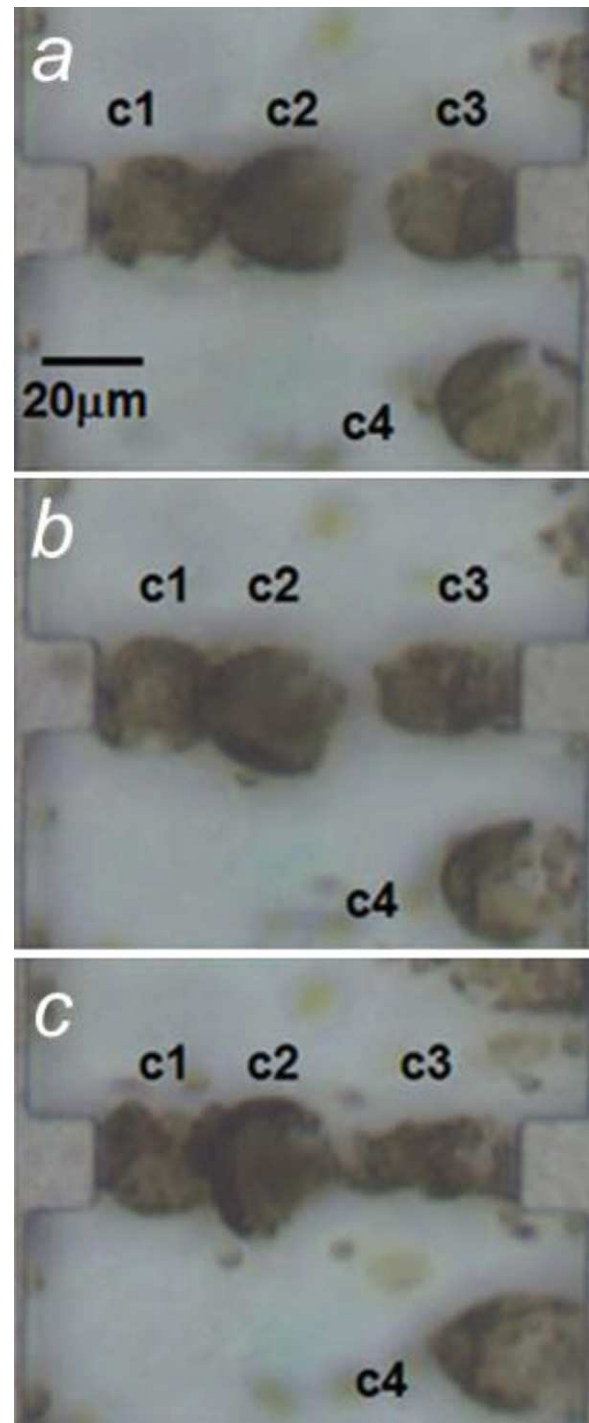


Fig. 15. Alignment of tobacco mesophyll protoplasts at $V_{p-p} = 4\text{ V}$ (a), 6 V (b), and 8 V (c). (a) Cells c1 and c2 form a pearl chain. (b) Cells c1 and c2 form a pearl chain and cell c3 starts to deform. (c) Cells c1, c2, and c3 form a pearl chain, then break and release their cytoplasm. Adapted with permission from Ref. [79].

With further increase in the voltage ($V_{p-p} \geq 8\text{ V}$), the mesophyll protoplasts were found to collapse completely, as shown in Fig. 15. After the rupture, the cytoplasm was released and affected the ion concentration of the buffer solution and hence, reduced the efficiency of cell pairing [79]. Thus, the use of DEP force for cell pairing may also ruin the cell structure when the applied electric field is very high. The experimental result shows that $V_{rms} = 3\text{--}4\text{ V}$ is safe for most cells. And excessive cell deformation during electrofusion is not desirable as it may damage the cell membrane structure, and

hence can become harmful for cell viability. In addition, plant protoplasts are easier to be broken than animal cells due to their lower deformability. Besides cell pairing, electrodeformation also affects the cell membrane electrical breakdown. Electric stress and elongation forces in electrodeformation, which are evolved from the transient polarization of the cytosol, are predominantly responsible for the enhanced electroporation of the membranes in low-conductivity media and also helpful to cell electrofusion. It enlarges the breakdown area on the membrane and improves the electrofusion performance [108–110].

Since cell electrofusion depends on the reversible electroporation, the parameters of the imposed DC pulses, including intensity, duration, and pulse number, generally affect the electrofusion efficiency and viability of formed hybrid cells [40,111,112]. Reversible electroporation occurs when the electric field reaches the threshold value for breakdown of the membrane. Electroporation can be easily accomplished under higher electric field, but in that scenario, the cell viability will be decreased because of the manifestation of irreversible electroporation at very strong field. It has been observed that when the applied field is increased from 600 to 1200 V/cm, although the electrofusion efficiency increases from ~20% to ~40%, the percentage of viable cells decreases from ~90% to ~10% [48]. Similarly, Clow et al. [73] reported that the fusion of cell couplets generally occurs at voltages around 110–120 V, whereas the cell lysis occurs at 160 V. Thus, adoption of suitable electric field intensity is important for high efficient electrofusion while the formed hybrid cells have high viable rate. The duration of pulses also has important influence to the cell fusion efficiency. Wang and Lu [48] reported that the pulse width (also the time of cell couplets flowing through the narrow section of the microfluidic channel) affects both the fusion efficiency and viable rate of the fused hybrid cells when the field intensity varies between 600 and 1000 V/cm [48]. As expected, longer duration pulse resulted in higher fusion efficiency [113], whereas the viable rate decreases with an increase in the pulse duration. Typically, multiple pulses resulted in higher fusion efficiency than single pulse. However, the fusion efficiencies under three DC pulses of 50 μ s and six DC pulses of 100 μ s are found to be $24 \pm 11\%$ and $22 \pm 13\%$, respectively [94], and the fusion efficiencies have no significant difference under the two conditions. On the other hand, the mechanism of cell fusion using AC signal is complicated. Some researchers indicated that AC field can prone the plasma membrane for electrofusion by generating protein free areas in the cell membrane. But observations of Sowers [114] contradict this notion, indicating that the effect of AC signal on the cell fusion is still not clear. But in the study by Kemna et al. [94], significant increase in fusion efficiency was observed when an AC field is applied before and after the DC pulses. This shows that the AC signal does have some unknown effect on the cell fusion process. We speculate that, most probably the AC signal induces the positive DEP force to ensure that the two cells are always in close contact to get stable environment for cytoplasm exchange and membrane reconstruction for efficient electrofusion [47].

4.3. Cell types

In recent studies, different kinds of cells are used in experiments, such as mammalian cells, microorganism cells, and the plant cytoplasts. In plant cytoplast studies, researchers found that plant cytoplasts are easily fused due to the large diameter and the low deformability of the cell membrane. As mentioned earlier, experimental results show that an excessive AC field in cell pairing process can induce breakout of the plant cytoplast. Human cells, such as HEK293 cells, K562 cells, and Jurkat cells, attracted more attention due to the widespread applications and great potential on the treatments of human diseases. Especially, the electrofusion studies on somatic cells and stem cells show great potential in the

epigenetic reprogramming of somatic cells. The NIH3T3 cells and the mESC cells [83,93], the oocyte and somatic donor cells [49,73] are also used to form hybrid cells on microfluidic chips. In these studies, more attention is needed for the electrofusion of two different kinds of cells, with significantly different diameters, as membrane voltage depends linearly on the cell diameter. Since the reversible electroporation occurs at a membrane voltage around 1 V [87,115], cells with smaller diameter are reversibly electroporated while the larger cell could have been broken in that situation. For example, with the pulse duration of 100–300 ms, irreversible electroporation occurred at 300–400, 400–500, and 1100–1200 V/cm for M109 tumor cells, white blood cells, and red blood cells, respectively [116].

Pre-treatment of cells is another important factor for efficient cell-electrofusion. For example, the study on electrofusion between B cells and NS-1 cells shows that the electrofusion efficiency for un-treated and treated NS-1 cells with pronase are, respectively, $22 \pm 13\%$, and $51 \pm 11\%$ [94]. The result of electrofusion between B cells and un-treated NS-1 cells shows that most cell-pairs only have dye transfer without clear membrane reorganization. On the other hand, NS-1 cells treated with pronase are more stable under higher field strengths and longer exposure times, yielding a higher survival rate after applying DC pulses for fusion, and most cell-pairs have membrane reorganization. With all the above discussion, it becomes clear that the types of the cells used for fusion significantly affect the overall electrofusion performance, because the dielectrophoretic force and membrane voltage depend on the cell diameter, which further depend on the cell type. As mentioned earlier, for the same external electric field, bigger cells have higher membrane voltage, thus are easier to be electroporated at lower electrical field [116]. Therefore, it is necessary to design and fabricate more novel microstructures, like micro-pit, micro-trap and micro-orifice to modify the electric field distribution for similar trans-membrane potential formation at the contact point between two cells with significantly different diameters.

4.4. Osmolarity of buffer solution

The characteristics of buffer solution, especially osmolarity, also showed significant influence on the efficiency of electrofusion. Generally, cell diameter varies with the osmolarity, and therefore, the corresponding operating voltage for electroporation also varies with the osmolarity, leading to a variation in the electrofusion efficiency. For example, in the fusion of donor cells and oocyte, somatic cell's size increases about 20% in hypoosmolar buffer medium [73]. The required voltages for electroporation of HEK293 cells in the hypotonic buffer (0.2 mol/L mannitol), isotonic buffer (0.3 mol/L mannitol), and the hypertonic buffer (0.4 mol/L mannitol) are, respectively, 12–13 V, 14–16 V, and 20 V, and their corresponding electrofusion efficiencies are, 33%, 55% and 28%, respectively [79]. The 'break ratio' (defined as the ratio of the number of broken cells to the total number of cells during the entire fusion process), in the above-mentioned three conditions are found to be around 15%, 8%, and 6%, respectively. These results show that cells generally swell in buffer with low osmolarity, therefore a lower voltage is required for electroporation in buffer with lower osmolarity. Although cell size increase in hypotonic media reduces the electroporation voltage, excessively low osmolarity may also induce cell rupture and damage of hybrid cells. However, Usaj et al. [117] shows that higher fusion yields in hypotonic media is not caused by hypotonic treatment affection on the cell electroporation. This prediction is based on the fact that the cell permeabilization is on the same degree for a given ITV (Induced Transmembrane Voltage) both in isotonic and hypotonic environments. In addition, this research suggests that better electrofusion performance is indeed induced by the beneficial hypotonic affection on membrane–membrane interactions,

like improved physical cell contacts or enhanced fusogenic state of the cell membrane in hypotonic surrounding media [117].

Various groups used sucrose, sorbitol, and mannitol to adjust the osmolarity since these materials do not affect the ionic concentration of the buffer solution during the cell pairing and (or) electrofusion processes [79]. However, the sugar composition of the hypotonic pulse media (trehalose, sorbitol or inositol) significantly affects the cell electrofusion [118]. The sugar composition of hypotonic pulse media changes the cellular volume before electroporation. For example, the disaccharide trehalose generally allowed regulatory volume decrease (RVD). In contrast, inhibited RVD or even induced secondary swellings are always induced by the monomeric sugar alcohols like sorbitol and inositol. Selectivity of volume-sensitive channels (VSC) in the different types of cell membranes can induce completely dissimilar volume responses. Considering the relativity between cellular volume and electrofusion, 2 min pretreatment in hypotonic surrounding media can mostly produce highest fusion efficiency. However, excessively long hypotonic treatment (10–20 min) may reduce viability of hybrid cell. The viability reduction is properly caused by the reduction of cell size upon RVD induced by the trehalose, or the excessive loss of cytosolic electrolytes through VSC due to inositol/sorbitol [118].

5. Future trends

Traditional electrofusion systems and most microfluidic electrofusion devices do not consider separation of hybrid cells from the mixture with un-fused cells after the cell fusion process. Only microfluidic devices with the micro-orifice structures can realize the cell separation function to some extent by eliminating the cell pairing between the same types of cells since the insulating wall with micro-orifices can prevent cell exchange between two channels. The electric field constriction ensures that the electroporation occurs only at the contact point between two paired cells. However, extraction of the formed hybrid cells at the small micro-orifices is not convenient, and squeezing the hybrid cells through the micro-orifices can potentially damage the hybrid cells. Also the cytoplasm exchange and nucleus fusion are affected by the size of the micro-orifice. Therefore, the issue related to the separation of hybrid cells from the mixture is still not resolved properly and considerable attention is needed in this direction. In the existing fusion studies, separation is accomplished by the chemical or biological techniques, such as FACS [119–121], MACS [122–125], and HAT screening [126]. The FACS can rapidly separate cells in a buffer solution by detecting the size and the color of cell fluorescence. The advantage of this method is high throughput, which reaches almost 300,000 cells per minute, and there is no damage in the separation process. The HAT screening needs pre-modification of the cells for electrofusion. And the mixture of the hybrid cells and un-fused cells after electrofusion process needs to be cultured in the selective medium [94]. The MACS is another separation method, which allows cell to be separated by the antibodies against a particular surface antigen. In this case, the cells are pre-modified with magnetic nanoparticles coated with antibodies. During fusion process, three types of cells are generated: (i) hybrid cells fused with two different types of cells, (ii) un-fused cells and (iii) hybrid cells fused by two same types of cells. Each of these cells generally expresses different types of antigens because of their pre-treatments with antibody-coated magnetic nanoparticles. Therefore, with proper detection method, the desired hybrid cells fused with two different types of cells are separated from the mixture.

Recently, many new on-chip cell sorting or separation techniques have been developed. Compared with the conventional sorting technology, a chip-based cell sorter has several advantages,

such as low cost, small sample volume, high speed analysis, and good portability [127]. On chip cell sorting or separation can be realized by the same FACS, MACS and electrokinetics-based cell sorting techniques discussed earlier. Recently, a micro fluorescence-activated cell sorter (microFACS) with integrated piezoelectric actuator and optofluidic waveguide on a chip is developed for high sensitivity, high throughput cell separation [128–130]. Under a high flow rate (~ 10 cm/s), the sorting process automatically runs in high throughput by using the field programmable gate array (FPGA) and real time control loop system. Also the sensitivity of the system is enhanced by using a Teflon AF coated liquid core waveguide (LCW) structure, and the sensitivity is found to be much higher than the conventional FACS system [130]. The preliminary results show that the sorting efficiency is about 70% with no false sorting [128], and the throughput of this low power (<1 mW) microFACS is ~ 1500 cells per second [129]. Therefore, the integration of this microFACS component into the electrofusion microfluidic platform will improve the automation of cell fusion and separation.

In addition to cell separation, a complete cell electrofusion process with chip-based hybrid cell culture function is also very important for automatic operation and anti-pollution of the cell electrofusion process. With the development of the on-chip cell culture technology, the microfluidic chip can create a controllable microenvironment for cell culture by integrating micro-pump, self-contained flow loops, and microvalves, and various other microstructures/micro-components. It will be helpful to improve the cell viability. However, only a few reports considered cell culture within the cell electrofusion microfluidic device. For example, Skelley et al. [93] developed a microfluidic device, within which cells are cultured for 3 days. Apparently, the culture result shows that this microfluidic device has good cell culture ability. Therefore this report shows great potential in cell-pairing, -fusion and -culture on the same microfluidic platform. Similarly, micro-orifice based microfluidic device also shows the capability of on-chip culturing ability of hybrid cells. For example, hybrid cells, formed at the micro-orifices, show cell division on the PDMS chip after loading the cell growth medium [46,88]. When the micro-orifice is bigger, the fusants escaping from the orifice are divided into two or three daughter cells in 48 h, and the daughter cells can further be divided into either three or two in 72 h. When the micro-orifice is too small, the fusants cannot escape from the orifice until mitotic cell division phase occurs. In this case, the fusant is divided into 4 daughter cells. The experiments show that this microfluidic chip has the on chip culture ability to some extent, but the exchange between two parent cells of the fusant is not complete, which may affect the performance of the daughter cells. For a complete realization of all the cell culture processes (such as cell seeding, growth, detachment, and re-seeding on fresh surface), within a single microfluidic platform, the application of digital microfluidics (DMF) can be very useful [131]. Therefore, the integration of cell electrofusion and cell culture in one microfluidic platform is highly desirable for diverse device application. On the flow-through microfluidic system developed by Kirschbaum et al. [71], a complete cell electrofusion procedure including cell characterization, identification, selection, pairing, electroporation, fusion, further cultivation and analysis has been realized by optical control. The integration of single-cell electrofusion function allows one to produce fusants, conduct systematic study on correlation between experimental conditions and the resulting fusion efficiency, cell viability, cell proliferation, and cell differentiation. In accordance with this trend, the future cell electrofusion system should have all the following functions in one system: cell pairing, reversible cell electroporation, nucleus fusion, hybrid cell separation and culture. With these capabilities, the cell viability, automation, reliability and stain-resistant ability can be improved enormously.

6. Conclusions

Many microfluidic devices aimed at the cell electrofusion process, especially at the cell pairing and cell fusion, have been developed in recent years. In this article, the latest microfluidic cell electrofusion devices were reviewed. Compared with conventional cell pairing methods, some novel manipulation techniques were applied on the microfluidic device, such as chemical conjugation, electric field, and microfluidic controlling based on microstructures. These new methods can control cells paired as one-to-one, especially one-to-one heterogeneous cell pairs in high efficiency. It eliminates the undesired multi-cell fusion or homologous cell fusion. In addition, research on cell electrofusion focused on electric field distribution optimization for better electrofusion efficiency. High strength electric field induced by high aspect-ratio microelectrodes or electric field constriction based on microstructures shows great potential in high-yield electrofusion. The local electric field constriction also reduces the Joule heating effect and improves the cell viability. Although most microfluidic devices just considered the cell pairing and electrofusion, the integration of microfluidic cell separation and cell culture processes with the cell electrofusion process is recommended in the future. A fully automated lab-on-a-chip cell-electrofusion device with the functions of cell pairing, electrofusion, hybrid cell separation and culture is expected to improve the cell viability, reliability and stain-resistant ability.

Acknowledgement

This work is supported by the World Class University Grant R32-2008-000-20082-0 of the National Research Foundation of Korea.

References

- [1] J. Fulka, P. Loi, H. Fulka, G. Ptak, T. Nagai, Nucleus transfer in mammals: non-invasive approaches for the preparation of cytoplasts, *Trends in Biotechnology* 22 (2004) 279–283.
- [2] M. Kato, E. Sasamori, T. Chiba, Y. Hanyu, Cell activation by CpG ODN leads to improved electrofusion in hybridoma production, *Journal of Immunological Methods* 373 (2011) 102–110.
- [3] Z.Y. Li, X.S. Sun, J. Chen, X.M. Liu, S.M. Wisely, Q. Zhou, J.P. Renard, G.H. Leno, J.F. Engelhardt, Cloned ferrets produced by somatic cell nuclear transfer, *Developmental Biology* 293 (2006) 439–448.
- [4] B.C. Sarkhel, S.M. Daniel, P. Raipuria, Efficiency of cloned embryo production using different types of cell donor and electric fusion strengths in goats, *Small Ruminant Res.* 77 (2008) 45–50.
- [5] K. Wang, Z. Beyhan, R.M. Rodriguez, P.J. Ross, A.E. Lager, G.G. Kaiser, Y. Chen, J.B. Cibelli, Bovine ooplasm partially remodels primate somatic nuclei following somatic cell nuclear transfer, *Cloning and Stem Cells* 11 (2009) 187–202.
- [6] I. Wilmut, A.E. Schnieke, J. McWhir, A.J. Kind, K.H. Campbell, Viable offspring derived from fetal and adult mammalian cells, *Nature* 385 (1997) 810–813.
- [7] D.J. Ambrosi, B. Tanasijevic, A. Kaur, C. Obergfell, R.J. O'Neill, W. Krueger, T.P. Rasmussen, Genome-wide reprogramming in hybrids of somatic cells and embryonic stem cells, *Stem Cells* 25 (2007) 1104–1113.
- [8] C.A. Cowan, J. Atienza, D.A. Melton, K. Eggan, Nuclear reprogramming of somatic cells after fusion with human embryonic stem cells, *Science* 309 (2005) 1369–1373.
- [9] C.A. Cowan, I. Klimanskaya, J. McMahon, J. Atienza, J. Witmyer, J.P. Zucker, S. Wang, C.C. Morton, A.P. McMahon, D. Powers, D.A. Melton, Derivation of embryonic stem-cell lines from human blastocysts, *New England Journal of Medicine* 350 (2004) 1353–1356.
- [10] M. Tada, Y. Takahama, K. Abe, N. Nakatsuji, T. Tada, Nuclear reprogramming of somatic cells by in vitro hybridization with ES cells, *Current Biology* 11 (2001) 1553–1558.
- [11] E.H. Chen, E.N. Olson, Unveiling the mechanisms of cell-cell fusion, *Science* 308 (2005) 369–373.
- [12] A. Biragyn, K. Tani, M.C. Grimm, S. Weeks, L.W. Kwak, Genetic fusion of chemokines to a self tumor antigen induces protective, T-cell dependent antitumor immunity, *Nature Biotechnology* 17 (1999) 253–258.
- [13] J.M. Melancon, T.P. Foster, K.G. Kousoulas, Genetic analysis of the herpes simplex virus type 1 UL20 protein domains involved in cytoplasmic virion envelopment and virus-induced cell fusion, *Journal of Virology* 78 (2004) 7329–7343.
- [14] X.C. Yu, P.A. McGraw, F.S. House, J.E. Crowe, An optimized electrofusion-based protocol for generating virus-specific human monoclonal antibodies, *Journal of Immunological Methods* 336 (2008) 142–151.
- [15] S.K. Dessain, S.P. Adekar, J.B. Stevens, K.A. Carpenter, M.L. Skorski, B.L. Barnoski, R.A. Goldsby, R.A. Weinberg, High efficiency creation of human monoclonal antibody-producing hybridomas, *Journal of Immunological Methods* 291 (2004) 109–122.
- [16] R.J. Orentas, D. Schauer, Q. Bin, B.D. Johnson, Electrofusion of a weakly immunogenic neuroblastoma with dendritic cells produces a tumor vaccine, *Cell Immunol.* 213 (2001) 4–13.
- [17] B.D. Hock, G. Roberts, J.L. McKenzie, P. Gokhale, N. Salm, A.D. McLellan, N.W. Patton, J.A. Roake, Exposure to the electrofusion process can increase the immunogenicity of human cells, *Cancer Immunol. Immun.* 54 (2005) 880–890.
- [18] V.L. Sukhorukov, R. Reuss, J.M. Endter, S. Fehrmann, A. Katsen-Globa, P. Gessner, A. Steinbach, K.J. Müller, A. Karpas, U. Zimmermann, H. Zimmermann, A biophysical approach to the optimisation of dendritic-tumour cell electrofusion, *Biochemical and Biophysical Research Communications* 346 (2006) 829–839.
- [19] K.T. Trevor, C. Cover, Y.W. Ruiz, E.T. Akporiaye, E.M. Hersh, D. Landais, R.R. Taylor, A.D. King, R.E. Walters, Generation of dendritic cell-tumor cell hybrids by electrofusion for clinical vaccine application, *Cancer Immunol. Immun.* 53 (2004) 705–714.
- [20] W.M. Siders, K.L. Vergilis, C. Johnson, J. Shields, J.M. Kaplan, Induction of specific antitumor immunity in the mouse with the electrofusion product of tumor cells and dendritic cells, *Mol. Ther.: J. Am. Soc. Gene Ther.* 7 (2003) 498–505.
- [21] E. Posfai, R. Kunzmann, V. Brochard, J. Salvaing, E. Cabuy, T.C. Roloff, Z.C. Liu, M. Tardat, M. van Lohuizen, M. Vidal, N. Beaujean, A.H.F.M. Peters, Polycomb function during oogenesis is required for mouse embryonic development, *Gene Dev.* 26 (2012) 920–932.
- [22] F. Sadeghian, S. Hosseinkhani, A. Alizadeh, A. Hatefi, Design, engineering and preparation of a multi-domain fusion vector for gene delivery, *International Journal of Pharmaceutics* 427 (2012) 393–399.
- [23] L.H. Li, M.L. Hensen, Y.L. Zhao, S.W. Hui, Electrofusion between heterogeneous-sized mammalian cells in a pellet: potential applications in drug delivery and hybridoma formation, *Biophysical Journal* 71 (1996) 479–486.
- [24] R. Jahn, T. Lang, T.C. Sudhof, Membrane fusion, *Cell* 112 (2003) 519–533.
- [25] R.A. Miller, F.H. Ruddle, Pluripotent teratocarcinoma-thymus somatic cell hybrids, *Cell* 9 (1976) 45–55.
- [26] Z.X. Zhang, Q.Z. Guan, Y.H. Guo, Y.X. Wei, F.Z. Meng, Regeneration of somatic hybrids of ginger via chemical protoplast fusion, *Plant Cell Tissue Org.* 102 (2010) 279–284.
- [27] A. Szczerbakowa, U. Maciejewska, P. Pawlowski, J.S. Skierski, B. Wielgat, Electrofusion of protoplasts from *Solanum tuberosum*, *S. nigrum* and *S. bulbocastanum*, *Acta Physiol. Plant.* 23 (2001) 169–179.
- [28] M. Greplova, H. Polzerova, H. Vlastnikova, Electrofusion of protoplasts from *Solanum tuberosum*, *S-bulbocastanum* and *S-pinnatisectum*, *Acta Physiol. Plant.* 30 (2008) 787–796.
- [29] G. Kohler, C. Milstein, Continuous cultures of fused cells secreting antibody of predefined specificity, *Nature* 256 (1975) 495–497.
- [30] T. Nakamura, K.W. Peng, S. Vongpunsawad, M. Harvey, H. Mizuguchi, T. Hayakawa, R. Cattaneo, S.J. Russell, Antibody-targeted cell fusion, *Nature Biotechnology* 22 (2004) 331–336.
- [31] N. Zakai, R.G. Kulka, A. Loyter, Fusion of human erythrocyte ghosts promoted by the combined action of calcium and phosphate ions, *Nature* 263 (1976) 696–699.
- [32] Y. Okada, Analysis of giant polynuclear cell formation caused by HVJ virus from Ehrlich's ascites tumor cells. III. Relationship between cell condition and fusion reaction or cell degeneration reaction, *Experimental Cell Research* 26 (1962) 119–128.
- [33] T. Spencer, Action of Sendai virus and neuraminidase on the alkaline phosphatase isoenzymes of HeLa cells, *Nature* 215 (1967) 985–986.
- [34] J. White, K. Matlin, A. Helenius, Cell fusion by Semliki Forest, influenza, and vesicular stomatitis viruses, *Journal of Cell Biology* 89 (1981) 674–679.
- [35] U. Zimmermann, J. Vienken, G. Pilwat, W.M. Arnold, Electro-fusion of cells: principles and potential for the future, *Ciba Found Symp.* 103 (1984) 60–85.
- [36] J. Vienken, U. Zimmermann, H.P. Zenner, W.T. Coakley, R.K. Gould, Electroacoustic fusion of cells, *Naturwissenschaften* 72 (1985) 441–442.
- [37] U. Zimmermann, J. Vienken, Electric field-induced cell-to-cell fusion, *Journal of Membrane Biology* 67 (1982) 165–182.
- [38] J. Vienken, U. Zimmermann, Electric field-induced fusion: electro-hydraulic procedure for production of heterokaryon cells in high yield, *FEBS Letters* 137 (1982) 11–13.
- [39] P. Scheurich, U. Zimmermann, Electrically stimulated fusion of different plant cell protoplasts: mesophyll cell and guard cell protoplasts of vicia faba, *Plant Physiology* 67 (1981) 849–853.
- [40] U. Zimmermann, P. Scheurich, Fusion of *Avena sativa* mesophyll cell protoplasts by electrical breakdown, *Biochimica et Biophysica Acta* 641 (1981) 160–165.
- [41] R. Wiegand, G. Weber, K. Zimmermann, S. Monajembashi, J. Wolfrum, K.O. Greulich, Laser-induced fusion of mammalian cells and plant protoplasts, *Journal of Cell Science* 88 (Pt 2) (1987) 145–149.

- [42] R.W. Steubing, S. Cheng, W.H. Wright, Y. Numajiri, M.W. Berns, Laser induced cell fusion in combination with optical tweezers: the laser cell fusion trap, *Cytometry* 12 (1991) 505–510.
- [43] A. Stromberg, F. Ryttsen, D.T. Chiu, M. Davidson, P.S. Eriksson, C.F. Wilson, O. Orwar, R.N. Zare, Manipulating the genetic identity and biochemical surface properties of individual cells with electric-field-induced fusion, *Proceedings of the National Academy of Sciences of the United States of America* 97 (2000) 7–11.
- [44] U. Zimmermann, G.A. Neil, *Electromanipulation of Cells*, CRC Press, Boca Raton, FL, 1996.
- [45] D.C. Chang, Cell poration and cell fusion using an oscillating electric field, *Biophysical Journal* 56 (1989) 641–652.
- [46] M. Gel, Y. Kimura, O. Kurosawa, H. Oana, H. Kotera, M. Washizu, Dielectrophoretic cell trapping and parallel one-to-one fusion based on field constriction created by a micro-orifice array, *Biomicrofluidics* 4 (2010) 022808–0228088.
- [47] J. Yang, L.P. Zhao, Z.Q. Yin, N. Hu, J. Chen, T.Y. Li, I. Svir, X.L. Zheng, Chip-based cell electrofusion, *Advanced Engineering Materials* 12 (2010) B398–B405.
- [48] J. Wang, C. Lu, Microfluidic cell fusion under continuous direct current voltage, *Applied Physics Letters* 89 (2006).
- [49] A. Clow, P. Gaynor, B. Oback, Coplanar film electrodes facilitate bovine nuclear transfer cloning, *Biomedical Microdevices* 11 (2009) 851–859.
- [50] G.J. Cook, L.A. Babiuik, J.B. Hudson, Cell-fusion properties of Sendai virus prepared by polyethylene-glycol precipitation, *Canadian Journal of Microbiology* 18 (1972) 607–610.
- [51] J. Yang, M.H. Shen, Polyethylene glycol-mediated cell fusion, *Methods in Molecular Biology* 325 (2006) 59–66.
- [52] T.H. Norwood, C.J. Zeigler, G.M. Martin, Dimethyl sulfoxide enhances polyethylene glycol-mediated somatic cell fusion, *Somatic Cell Genetics* 2 (1976) 263–270.
- [53] Y. Wakita, S. Yokota, N. Yoshizawa, T. Katsuki, Y. Nishiyama, T. Yokoyama, M. Fukui, H. Sasamoto, Interfamilial cell fusion among leaf protoplasts of *Populus alba*, *Betula platyphylla* and *Alnus firma*: assessment of electric treatment and in vitro culture conditions, *Plant Cell Tissue Org.* 83 (2005) 319–326.
- [54] M. Usaj, K. Trontelj, D. Miklavcic, M. Kanduser, Cell-cell electrofusion: optimization of electric field amplitude and hypotonic treatment for mouse melanoma (B16-F1) and Chinese Hamster ovary (CHO) cells, *Journal of Membrane Biology* 236 (2010) 107–116.
- [55] J. Vienken, U. Zimmermann, M. Fouchard, D. Zagury, Electrofusion of myeloma cells on the single cell level. Fusion under sterile conditions without proteolytic enzyme treatment, *FEBS Letters* 163 (1983) 54–56.
- [56] J. Vienken, U. Zimmermann, An improved electrofusion technique for production of mouse hybridoma cells, *FEBS Letters* 182 (1985) 278–280.
- [57] K.L. White, in: J.A. Nickoloff (Ed.), *Methods in Molecular Biology*, vol. 47, Humana, Totawa, NJ, 1995, pp. 283–294.
- [58] T.C. Bakker Schut, Y.M. Kraan, W. Barlag, L. de Leij, B.G. de Grooth, J. Greve, Selective electrofusion of conjugated cells in flow, *Biophysical Journal* 65 (1993) 568–572.
- [59] B. Oback, D.N. Wells, Cloning cattle, *Clon. Stem Cells* 5 (2003) 243–256.
- [60] B. Oback, A.T. Wiersema, P. Gaynor, G. Laible, F.C. Tucker, J.E. Oliver, A.L. Miller, H.E. Troskie, K.L. Wilson, J.T. Forsyth, M.C. Berg, K. Cockrem, V. McMillan, H.R. Terwit, D.N. Wells, Cloned cattle derived from a novel zona-free embryo reconstruction system, *Clon. Stem Cells* 5 (2003) 3–12.
- [61] T.B. Jones, *Electromechanics of Particles* (digitally printed first pbk. ed.), Cambridge University Press, Cambridge, New York, 2005.
- [62] C.S. Chen, H.A. Pohl, Biological dielectrophoresis: the behavior of lone cells in a nonuniform electric field, *Annals of the New York Academy of Sciences* 238 (1974) 176–185.
- [63] H.A. Pohl, J.S. Crane, Dielectrophoresis of cells, *Biophysical Journal* 11 (1971) 711–727.
- [64] B. Sankaran, M. Racic, A. Tona, M.V. Rao, M. Gaitan, S.P. Forry, Dielectrophoretic capture of mammalian cells using transparent indium tin oxide electrodes in microfluidic systems, *Electrophoresis* 29 (2008) 5047–5054.
- [65] K.S. Yun, H. Park, D. Kim, Single-cell manipulation on microfluidic chip by dielectrophoretic actuation and impedance detection, *Sens. Actuators B Chem.* 150 (2010) 167–173.
- [66] T. Yasukawa, M. Suzuki, H. Shiku, T. Matsue, Control of the microparticle position in the channel based on dielectrophoresis, *Sens. Actuators B Chem.* 142 (2009) 400–403.
- [67] K. Khoshmanesh, S. Nahavandi, S. Baratchi, A. Mitchell, K. Kalantar-zadeh, Dielectrophoretic platforms for bio-microfluidic systems, *Biosensors and Bioelectronics* 26 (2011) 1800–1814.
- [68] T. Schnelle, T. Müller, G. Gradl, S.G. Shirley, G. Fuhr, Dielectrophoretic manipulation of suspended submicron particles, *Electrophoresis* 21 (2000) 66–73.
- [69] C. Reichle, K. Sparbier, T. Müller, T. Schnelle, P. Walden, G. Fuhr, Combined laser tweezers and dielectric field cage for the analysis of receptor–ligand interactions on single cells, *Electrophoresis* 22 (2001) 272–282.
- [70] T. Schnelle, T. Müller, S. Fiedler, G. Fuhr, The influence of higher moments on particle behaviour in dielectrophoretic field cages, *Journal of Electrostatics* 46 (1999) 13–28.
- [71] M. Kirschbaum, C.R. Guernth-Marschner, S. Cherre, A. de Pablo Pena, M.S. Jaeger, R.A. Kroczeck, T. Schnelle, T. Mueller, C. Duschl, Highly controlled electrofusion of individually selected cells in dielectrophoretic field cages, *Lab Chip* 12 (2012) 443–450.
- [72] T. Müller, G. Gradl, S. Howitz, S. Shirley, T. Schnelle, G. Fuhr, A 3-D microelectrode system for handling and caging single cells and particles, *Biosensors and Bioelectronics* 14 (1999) 247–256.
- [73] A.L. Clow, P.T. Gaynor, B.J. Oback, A novel micropit device integrates automated cell positioning by dielectrophoresis and nuclear transfer by electrofusion, *Biomedical Microdevices* 12 (2010) 777–786.
- [74] G. Tresset, S. Takeuchi, A microfluidic device for electrofusion of biological vesicles, *Biomedical Microdevices* 6 (2004) 213–218.
- [75] N. Hu, J. Yang, S. Qian, S.W. Joo, X. Zheng, A cell electrofusion microfluidic device integrated with 3D thin-film microelectrode arrays, *Biomicrofluidics* 5 (2011) 34121–3412112.
- [76] N. Hu, J. Yang, W.S. Hou, X.L. Zheng, Y. Cao, J. Yang, R. Xu, R.Q. Zhang, SOI-based cell electrofusion chip, *Chem. J. Chin. U.* 30 (2009) 42–45.
- [77] N. Hu, J. Yang, X.L. Zheng, Z.Q. Yin, H.W. Xu, X.G. Zhang, Y. Cao, J. Yang, B. Xia, R. Xu, J.W. Yan, F. Jiang, Polyimide membrane based flexible cell-electrofusion chip, *Chin. J. Anal. Chem.* 37 (2009) 1247–1250.
- [78] D.T. Chiu, A microfluidics platform for cell fusion—Commentary, *Current Opinion in Chemical Biology* 5 (2001) 609–612.
- [79] N. Hu, J. Yang, Z.Q. Yin, Y. Ai, S. Qian, I.B. Svir, B. Xia, J.W. Yan, W.S. Hou, X.L. Zheng, A high-throughput dielectrophoresis-based cell electrofusion microfluidic device, *Electrophoresis* 32 (2011) 2488–2495.
- [80] J. Ju, J.M. Ko, H.C. Cha, J.Y. Park, C.H. Im, S.H. Lee, An electrofusion chip with a cell delivery system driven by surface tension, *J. Micromech. Microeng.* 19 (2009).
- [81] Y. Cao, J. Yang, Z.Q. Yin, H.Y. Luo, M. Yang, N. Hu, J. Yang, D.Q. Huo, C.J. Hou, Z.Z. Jiang, R.Q. Zhang, R. Xu, X.L. Zheng, Study of high-throughput cell electrofusion in a microelectrode-array chip, *Microfluid Nanofluid* 5 (2008) 669–675.
- [82] N. Hu, J. Yang, S. Qian, X. Zhang, S.W. Joo, X. Zheng, A cell electrofusion microfluidic chip using discrete coplanar vertical sidewall microelectrodes, *Electrophoresis* 33 (2012) 1980–1986.
- [83] Y. Qu, N. Hu, H.W. Xu, J. Yang, B. Xia, X.L. Zheng, Z.Q. Yin, Somatic and stem cell pairing and fusion using a microfluidic array device, *Microfluid Nanofluid* 11 (2011) 633–641.
- [84] M. Kirschbaum, M.S. Jaeger, C. Duschl, Correlating short-term Ca²⁺ responses with long-term protein expression after activation of single T cells, *Lab Chip* 9 (2009) 3517–3525.
- [85] M. Kirschbaum, M.S. Jaeger, T. Schenkel, T. Breinig, A. Meyerhans, C. Duschl, T cell activation on a single-cell level in dielectrophoresis-based microfluidic devices, *Journal of Chromatography A* 1202 (2008) 83–89.
- [86] S. Masuda, M. Washizu, T. Nanba, Novel method of cell fusion in field constriction area in fluid integration circuit, *IEEE Trans. Ind. Appl.* 25 (1989) 732–737.
- [87] B. Techaumnat, K. Tsuda, O. Kurosawa, G. Murat, H. Oana, M. Washizu, High-yield electrofusion of biological cells based on field tailoring by micro-fabricated structures, *IET Nanobiotechnol.* 2 (2008) 93–99.
- [88] M. Gel, S. Suzuki, Y. Kimura, O. Kurosawa, B. Techaumnat, H. Oana, M. Washizu, Microorifice-based high-yield cell fusion on microfluidic chip: electrofusion of selected pairs and fusant viability, *IEEE Trans. Nanobiosci.* 8 (2009) 300–305.
- [89] Y. Kimura, M. Gel, B. Techaumnat, H. Oana, H. Kotera, M. Washizu, Dielectrophoresis-assisted massively parallel cell pairing and fusion based on field constriction created by a micro-orifice array sheet, *Electrophoresis* 32 (2011) 2496–2501.
- [90] M. Radisic, R.K. Iyer, S.K. Murthy, Micro- and nanotechnology in cell separation, *Int. J. Nanomed.* 1 (2006) 3–14.
- [91] Y.J. Kang, D.Q. Li, S.A. Kalams, J.E. Eid, DC-dielectrophoretic separation of biological cells by size, *Biomedical Microdevices* 10 (2008) 243–249.
- [92] S.M. McFaul, B.K. Lin, H.S. Ma, Cell separation based on size and deformability using microfluidic funnel ratchets, *Lab Chip* 12 (2012) 2369–2376.
- [93] A.M. Skelley, O. Kirak, H. Suh, R. Jaenisch, J. Voldman, Microfluidic control of cell pairing and fusion, *Nature Methods* 6 (2009) 147–152.
- [94] E.W.M. Kemna, F. Wolbers, I. Vermes, A. van den Berg, On chip electrofusion of single human B cells and mouse myeloma cells for efficient hybridoma generation, *Electrophoresis* 32 (2011) 3138–3146.
- [95] C.T.S. Ching, T.P. Sun, W.T. Huang, S.H. Huang, C.S. Hsiao, K.M. Chang, A circuit design of a low-cost, portable and programmable electroproportion device for biomedical applications, *Sens. Actuators B Chem.* 166 (2012) 292–300.
- [96] D.C. Chang, T.S. Reese, Changes in membrane structure induced by electroproportion as revealed by rapid-freezing electron microscopy, *Biophysical Journal* 58 (1990) 1–12.
- [97] A. Stromberg, A. Karlsson, F. Ryttsen, M. Davidson, D.T. Chiu, O. Orwar, Microfluidic device for combinatorial fusion of liposomes and cells, *Analytical Chemistry* 73 (2001) 126–130.
- [98] J. Yang, Y. Cao, Z.Q. Yin, W.S. Hou, X.L. Zheng, N. Hu, J. Yang, R. Xu, R.Q. Zhang, Electric field simulation of high-throughput cell electrofusion chip, *Chin. J. Anal. Chem.* 36 (2008) 593–598.
- [99] B. Techaumnat, M. Washizu, Analysis of the effects of an orifice plate on the membrane potential in electroproportion and electrofusion of cells, *J. Phys. D Appl. Phys.* 40 (2007) 1831–1837.
- [100] M. Washizu, B. Techaumnat, Cell membrane voltage during electrical cell fusion calculated by re-expansion method, *Journal of Electrostatics* 65 (2007) 555–561.
- [101] M. Washizu, B. Techaumnat, Polarisation and membrane voltage of ellipsoidal particle with a constant membrane thickness: a series expansion approach, *IET Nanobiotechnol.* 2 (2008) 62–71.

- [102] R. Shirakashi, R. Reuss, A. Schulz, V.L. Sukhorukov, U. Zimmermann, Effects of a pulse electric field on electrofusion of Giant Unilamellar Vesicle (GUV)-Jurkat Cell (Measurement of fusion ratio and electric field analysis of pulsed GUV-Jurkat Cell), *J. Thermal Sci. Technol.* 7 (2012) 589–602.
- [103] K. Trontelj, M. Rebersek, M. Kanduser, V.C. Serbec, M. Sprohar, D. Miklavcic, Optimization of bulk cell electrofusion in vitro for production of human-mouse heterohybridoma cells, *Bioelectrochemistry* 74 (2008) 124–129.
- [104] X. Yu, P.A. McGraw, F.S. House, J.E. Crowe Jr., An optimized electrofusion-based protocol for generating virus-specific human monoclonal antibodies, *Journal of Immunological Methods* 336 (2008) 142–151.
- [105] M.C. Cole, P.J.A. Kenis, Multiplexed electrical sensor arrays in microfluidic networks, *Sens. Actuators B Chem.* 136 (2009) 350–358.
- [106] S.E. Yalcin, A. Sharma, S.Z. Qian, S.W. Joo, O. Baysal, On-demand particle enrichment in a microfluidic channel by a locally controlled floating electrode, *Sens. Actuators B Chem.* 153 (2011) 277–283.
- [107] Y. Xu, X. Hu, J. Liang, J. Sun, W. Gu, T. Zhao, Z. Wen, A microsystem of low-voltage-driven electrophoresis on microchip with array electrode pairs for the separation of amino acids, *Analytical and Bioanalytical Chemistry* 394 (2009) 1947–1953.
- [108] V.L. Sukhorukov, H. Mussauer, U. Zimmermann, The effect of electrical deformation forces on the electroporation of erythrocyte membranes in low- and high-conductivity media, *Journal of Membrane Biology* 163 (1998) 235–245.
- [109] K.A. Riske, R. Dimova, Electro-deformation and poration of giant vesicles viewed with high temporal resolution, *Biophysical Journal* 88 (2005) 1143–1155.
- [110] D.A. Stenger, K.V. Kaler, S.W. Hui, Dipole interactions in electrofusion. Contributions of membrane potential and effective dipole interaction pressures, *Biophysical Journal* 59 (1991) 1074–1084.
- [111] C.S. Djuzenova, V.L. Sukhorukov, G. Klock, W.M. Arnold, U. Zimmermann, Effect of electric field pulses on the viability and on the membrane-bound immunoglobulins of LPS-activated murine B-lymphocytes: correlation with the cell cycle, *Cytometry* 15 (1994) 35–45.
- [112] J.A. Kim, K.C. Cho, M.S. Shin, W.G. Lee, N.C. Jung, C.I. Chung, J.K. Chang, A novel electroporation method using a capillary and wire-type electrode, *Biosens. Bioelectron* 23 (2008) 1353–1360.
- [113] S. Talele, P. Gaynor, M.J. Cree, J. van Ekeran, Modelling single cell electroporation with bipolar pulse parameters and dynamic pore radii, *Journal of Electrostatics* 68 (2010) 261–274.
- [114] A.E. Sowers, Membrane electrofusion: a paradigm for study of membrane fusion mechanisms, *Methods in Enzymology* 220 (1993) 196–211.
- [115] O. Kurosawa, H. Oana, S. Matsuoka, A. Noma, H. Kotera, M. Washizu, Electroporation through a micro-fabricated orifice and its application to the measurement of cell response to external stimuli, *Measurement Science and Technology* 17 (2006) 3127–3133.
- [116] N. Bao, T.T. Le, J.X. Cheng, C. Lu, Microfluidic electroporation of tumor and blood cells: observation of nucleus expansion and implications on selective analysis and purging of circulating tumor cells, *Integr. Biol. UK* 2 (2010) 113–120.
- [117] M. Usaj, M. Kanduser, The systematic study of the electroporation and electrofusion of B16-F1 and CHO cells in isotonic and hypotonic buffer, *Journal of Membrane Biology* 245 (2012) 583–590.
- [118] V.L. Sukhorukov, R. Reuss, D. Zimmermann, C. Held, K.J. Muller, M. Kiesel, P. Gessner, A. Steinbach, W.A. Schenk, E. Bamberg, U. Zimmermann, Surviving high-intensity field pulses: strategies for improving robustness and performance of electrotransfection and electrofusion, *Journal of Membrane Biology* 206 (2005) 187–201.
- [119] M.B. Dainiak, A. Kumar, I.Y. Galaev, B. Mattiasson, *Methods in cell separations, Advances in Biochemical Engineering/Biotechnology* 106 (2007) 1–18.
- [120] D. Mattanovich, N. Borth, Applications of cell sorting in biotechnology, *Microb. Cell Fact.* 5 (2006) 12.
- [121] L.L. Du, J.J. Peng, G. Lin, G.X. Lu, The fusion of somatic cells and human embryonic stem cells by electrofusion method, *Cell Research* 18 (2008).
- [122] G. Dudin, E.W. Steegmayer, P. Vogt, H. Schnitzer, E. Diaz, K.E. Howell, T. Cremer, C. Cremer, Sorting of chromosomes by magnetic separation, *Hum Genet.* 80 (1988) 111–116.
- [123] R. Manz, M. Assenmacher, E. Pfluger, S. Miltenyi, A. Radbruch, Analysis and sorting of live cells according to secreted molecules, relocated to a cell-surface affinity matrix, *Proceedings of the National Academy of Sciences of the United States of America* 92 (1995) 1921–1925.
- [124] Y. Garbe, U. Klier, M. Linnebacher, Semiallogenic fusions of MSI(+) tumor cells and activated B cells induce MSI-specific T cell responses, *BMC Cancer* 11 (2011) 410.
- [125] H.N. Lode, R. Xiang, T. Dreier, N.M. Varki, S.D. Gillies, R.A. Reisfeld, Natural killer cell-mediated eradication of neuroblastoma metastases to bone marrow by targeted interleukin-2 therapy, *Blood* 91 (1998) 1706–1715.
- [126] J.W. Littlefield, Selection of hybrids from matings of fibroblasts in vitro and their presumed recombinants, *Science* 145 (1964) 709–710.
- [127] P.S. Dittich, P. Schwill, An integrated microfluidic system for reaction, high-sensitivity detection, and sorting of fluorescent cells and particles, *Analytical Chemistry* 75 (2003) 5767–5774.
- [128] S.H. Cho, C.H. Chen, F.S. Tsai, Y.H. Lo, Micro-fabricated fluorescence-activated cell sorter, *Conf. Proc. IEEE Eng. Med. Biol. Soc.* 2009 (2009) 1075–1078.
- [129] S.H. Cho, C.H. Chen, F.S. Tsai, J.M. Godin, Y.H. Lo, Human mammalian cell sorting using a highly integrated micro-fabricated fluorescence-activated cell sorter (microFACS), *Lab Chip* 10 (2010) 1567–1573.
- [130] A.Y. Fu, C. Spence, A. Scherer, F.H. Arnold, S.R. Quake, A microfabricated fluorescence-activated cell sorter, *Nature Biotechnology* 17 (1999) 1109–1111.
- [131] I. Barbulovic-Nad, S.H. Au, A.R. Wheeler, A microfluidic platform for complete mammalian cell culture, *Lab Chip* 10 (2010) 1536–1542.

Biographies

Dr. Ning Hu is a researcher in Key Laboratory of Biorheological Science and Technology and Key Laboratory for Optoelectronic Technology and Systems, Ministry of Education, in Chongqing University. He obtained his Ph.D. from Chongqing University in 2010. His research focuses on bio-MEMS, microfluidics, lab-on-a-chip technology, and cell electrofusion.

Dr. Jun Yang is a professor in Key Laboratory of Biorheological Science and Technology and Key Laboratory for Optoelectronic Technology and Systems, Ministry of Education, in Chongqing University. He obtained his Ph.D. from City University of Hong Kong in 2004. His research focuses on bio-MEMS, microfluidics, and biosensors.

Dr. Sang W. Joo received his PhD at the University of Michigan after his undergraduate and graduate degrees from Seoul National University. He then worked at Northwestern University, University of Illinois, and Wayne State University before he joined Yeungnam University. His research interest includes hydrodynamic stability, interfacial phenomena, and micro/nanofluidics. He is also the Director of WCU Nano Research Center.

Dr. Arghya Narayan Banerjee is an Assistant Professor in the School of Mechanical Engineering, Yeungnam University, Korea. After finishing his Ph.D. from Jadavpur University, India, he joined at University of Nevada and University of Colorado at Boulder, US before moving to Yeungnam University. His research interests include digital microfluidics/nanofluidics, nanomaterials for energy-related applications, thin film technology.

Dr. Shizhi Qian is an associate professor in Department of Mechanical and Aerospace Engineering, ODU, USA. He obtained his Ph.D. from University of Pennsylvania in 2004. His research focuses on electrokinetics; colloidal sciences; micro- and nanoscale transport; and micro/nanofluidics.